Does the Crowded Cell-like Environment Reduce the Chaperone-like Activity of α-Crystallin?

ARTICLE *in* BIOCHEMISTRY · NOVEMBER 2011

Impact Factor: 3.02 · DOI: 10.1021/bi201030y · Source: PubMed

8 AUTHORS, INCLUDING:

Natalia A Chebotareva
Russian Academy of Sciences
115 PUBLICATIONS **1,189** CITATIONS
SEE PROFILE

Serguey Yurievich Kleimenov
Russian Academy of Sciences
47 PUBLICATIONS **472** CITATIONS
SEE PROFILE

Konstantin O Muranov
Russian Academy of Sciences
78 PUBLICATIONS **506** CITATIONS
SEE PROFILE

Boris Kurganov
Russian Academy of Sciences
342 PUBLICATIONS **3,140** CITATIONS
SEE PROFILE

BIOCHEMISTRY
including biophysical chemistry & molecular biology

Article

pubs.acs.org/biochemistry

Does the Crowded Cell-like Environment Reduce the Chaperone-like Activity of α-Crystallin?

Svetlana G. Roman,*[,†,‡] Natalia A. Chebotareva,*[,†] Tatyana B. Eronina,[†] Sergey Yu. Kleymenov,[†,§] Valentina F. Makeeva,[†] Nikolay B. Poliansky,[∥] Konstantin O. Muranov,[∥] and Boris I. Kurganov[†]

[†]Bach Institute of Biochemistry, Russian Academy of Sciences, Leninsky pr. 33, Moscow 119071, Russia

[‡]Department of Physics, Moscow State University, Leninskie Gory, Moscow 119992, Russia

[§]Kol'tsov Institute of Developmental Biology, Russian Academy of Sciences, Vavilova st. 26, Moscow 119991, Russia

[∥]Emanuel Institute of Biochemical Physics, Russian Academy of Sciences, Kosygin st. 4, Moscow 119991, Russia

Supporting Information

ABSTRACT: The effect of crowding on the chaperone-like activity of α-crystallin has been studied using aggregation of UV-irradiated glycogen phosphorylase *b* (Ph*b*) from rabbit skeletal muscle as an aggregation test system. The merit of this test system is the possibility of testing agents that directly affect the stage of aggregation of the protein molecules. It was shown that the solution of Ph*b* denatured by UV contained aggregates with a hydrodynamic radius of 10.4 nm. These aggregates are relatively stable at 20 °C; however, they reveal a tendency to stick further in the presence of crowding agents. The study of the effect of α-crystallin on the aggregation of UV-irradiated Ph*b* in the presence of the crowding agents by dynamic light scattering at 37 °C showed that under crowding conditions the antiaggregation ability of α-crystallin was weakened. On the basis of the analytical ultracentrifugation, size-exclusion chromatography, and sodium dodecyl sulfate−polyacrylamide gel electrophoresis data, the scheme of interaction of UV-irradiated Ph*b* and α-crystallin has been proposed. It is assumed that chaperone−target protein complexes of two types are formed, namely, the complexes of dissociated forms of α-crystallin with a protein substrate and high-mass α-crystallin-denatured protein complexes. The complexes of the first type reveal a weak propensity to aggregate even under crowding conditions. The complexes of the second type are characterized by the lower rate of aggregation in comparison with that of original UV-irradiated Ph*b*. However, crowding stimulates the rate of aggregation of these complexes, resulting in the above-mentioned decrease in the chaperone-like activity of α-crystallin.

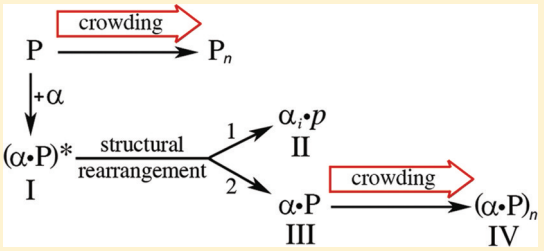

The cellular environment contains many volume-excluded macromolecules such as proteins, polysaccharides, nuclear acids, and lipids, creating conditions of so-called "crowding". Molecular crowding may significantly affect protein conformational transitions, protein folding, the rates of biochemical reactions, and association (aggregation) of macromolecules.[1−9]

Protein aggregation represents an essential problem for the living cells because it can potentially reduce the efficiency of protein folding and may provoke the formation of toxic aggregates.[4] When interpreting the effect of crowding on protein aggregation in model systems, we should realize that protein aggregation is a complex process involving conformational transitions of the monomer, the stage of nucleation, and stages of the growth of aggregates.[10−14] In general, the effect of crowders on the stage of the conformational transition in the monomer and the aggregation stages can be different; therefore, it is difficult to predict the net effect of excluded volume on protein aggregation. Besides, depending on the conditions, protein aggregation can lead to the formation of soluble oligomers, insoluble structureless amorphous aggregates, or highly ordered amyloid-like fibrils. Molecular crowding affects these different aggregation pathways in a different way. This was clearly demonstrated by Munishkina et al.,[11] who studied the effects of crowding on aggregation and fibrillation of four proteins: bovine *S*-carboxymethyl-α-lactalbumin (a disordered form of the protein with three of four disulfide bridges reduced), human insulin, bovine core histones, and human α-synuclein.

When the crowding effects in model systems are being studied, it is necessary to use a variety of different crowding agents to diminish the risk that observed effects are caused by specific interactions.[4] In this work, we used high-molecular mass crowders, polyethylene glycol (PEG) and Ficoll (70000 Da), as well as natural osmolyte trimethylamine *N*-oxide (TMAO). PEG fractions with a molecular mass in excess of a few thousand daltons reveal predominantly repulsive interactions with proteins and tend to provoke macromolecular association.[2,4,7,15,16] However, the repulsive excluded-volume PEG−protein interaction is compensated to some extent by attractive interaction between PEG and nonpolar regions on the surface of the protein molecule.[4,7,16] Ficoll, a crowder with a

Received: July 5, 2011
Revised: November 3, 2011
Published: November 7, 2011

polysaccharide nature, lacks such an attractive interaction with proteins. Ficoll−protein interactions can be described using pure excluded-volume models.[7]

In response to stress (osmotic, chemical, or thermal), many living organisms accumulate high concentrations of osmolytes. Osmolytes are small organic molecules, such as polyols, some amino acids, and methylamines. They protect proteins under stress conditions by stabilization of protein structure. The stabilizing effect is due to preferential exclusion of the osmolyte from the surface of the protein.[17,18] One of the osmolytes that are widely used as crowding agents in model experiments is TMAO.[2,5,11,19−22] It was shown in vivo that TMAO counteracts the damaging action of the excess of urea and salts and hydrostatic pressure on deep-water animals.[23−25] It should be noted that TMAO has a pK_a value of 4.66. The crowding action of TMAO is studied usually in the pH range of 6.0−8.0, where TMAO is almost neutral (zwitterionic form).

The main function of small heat-shock proteins (sHsps) is suppression of aggregation of partly or completely unfolded protein molecules in the cell. α-Crystallin, one of the representatives of the sHsp family, is a major protein of the vertebrate eye lens. This protein has been found in all tissues, including skeletal muscle.[26] Horwitz was the first to demonstrate the chaperone-like activity of α-crystallin.[27] According to current concepts, the chaperone-like activity of sHsps is due to the formation of the complexes between the unfolded protein and sHsp, these complexes being not prone to aggregation and retaining a target protein in a folding-competent form. Much evidence demonstrates the complexation of α-crystallin with nonnative proteins.[28−38] The main manifestation of the protective action of α-crystallin is an increase in the duration of the lag period on the kinetic curves of aggregation.[28,31,37,39−41]

One might expect that crowding would affect the chaperone-like activity of sHsps favoring the formation of sHsp−target protein complexes. Besides, the formed complexes might reveal a tendency to stick further in a crowded medium. Actually, the alterations of the antiaggregation activity of α-crystallin were registered in the presence of crowding agents. Ganea and Harding[42] showed that crowding agents, dextran (70000 Da) and PEG (8000 Da), decreased the α-crystallin chaperone-like activity of protecting glucose-6-phosphate dehydrogenase and malate dehydrogenase against glycation-induced inactivation. When studying the effect of dextran (68800 Da) on dithiothreitol-induced aggregation of ovotransferrin at various temperatures, Carver and co-workers[43] showed that α-crystallin and αA-crystallin were poorer chaperones under mimic crowding conditions. It is worth noting that Ghahghaei et al.[44] observed the diminution of the ability of αS-casein, a molecular chaperone found in bovine milk, to inhibit α-lactalbumin fibrillation in the presence of dextran (68000 Da). To establish the mechanism for a decrease in the chaperone-like activity of sHsps in crowded media, it is important to clarify the aggregation propensity of sHsp−target protein complexes.

The aim of this work was to study the effect of crowding on the chaperone-like activity of sHsps using α-crystallin as a molecular chaperone. We have elaborated a new test system that allows the study of the action of the agents being tested just on the stages of aggregation of denatured proteins. This system is based on aggregation of glycogen phosphorylase *b* (Ph*b*) denatured by ultraviolet (UV) radiation. The accelerating action of the crowding agents (PEG-20000, Ficoll-70000, and TMAO) on the aggregation of UV-irradiated Ph*b* was demonstrated. It was shown that the antiaggregation activity of α-crystallin estimated on the basis of measurements of the light scattering intensity was greatly reduced under crowding conditions. At rather high concentrations of the crowding agents, the complete loss of the chaperone-like activity of α-crystallin occurred. However, the data from analytical ultracentrifugation (AUC), size-exclusion chromatography (SEC), and SDS−PAGE show that α-crystallin may act as a protective agent because of the formation of the complex, including dissociated forms of α-crystallin and the protein substrate.

MATERIALS AND METHODS

Materials. Hepes, TMAO, glucose 1-phosphate, AMP, and Ficoll with a molecular mass of 70000 Da were purchased from Sigma. Dithiothreitol was purchased from ICN. PEG (20000 Da) was purchased from Ferak Berlin. NaCl was purchased from "Reakhim". Glycogen was purchased from "Olaine". All solutions for the experiments were prepared using deionized water obtained with the Easy-Pure II RF system (Barnstead).

Isolation and Purification of Ph*b*. Ph*b* was isolated from rabbit skeletal muscles by the method of Fisher and Krebs[45] using dithiothreitol instead of cysteine; the enzyme was crystallized four times. The preparations of Ph*b* were electrophoretically homogeneous. The Ph*b* concentration was determined spectrophotometrically at 280 nm using an absorption coefficient $A_{cm}^{1\%}$ of 13.2.[46]

Isolation of α-Crystallin. Purification of α-crystallin was performed from freshly excised lenses of 2-year-old steers according to the procedure described previously.[47] The concentration of α-crystallin was determined spectrophotometrically at 280 nm using an absorption coefficient $A_{cm}^{1\%}$ of 8.5.[48]

UV Irradiation of Ph*b*. UV irradiation of Ph*b* (1.5 mg/mL) was conducted in a 1 cm path quartz cell at 10 °C. A high-pressure Hg lamp (DRK-120, 120 W) was used in the irradiation experiments. A filter that passes UV light (270−390 nm) while blocking other wavelengths in the light spectrum was applied. The power of incident light was 5 mW/cm^2. The samples of UV-irradiated Ph*b* were centrifuged at 6800*g* for 5 min (10 °C).

Assay of Ph*b*. The enzymatic activity of Ph*b* was determined by the turbidimetric method[49,50] on the basis of the registration of the increase in glycogen solution absorbance at 360 nm using 1 cm cuvettes and a ThermoSpectronic model Genesys 6 spectrophotometer equipped with a thermostatically controlled cell. Spectrophotometric data were recorded to an IBM-compatible computer. The kinetics of the enzymatic reaction was registered at 30 °C in 0.08 M Hepes-NaOH buffer (pH 6.8) containing 0.1 M NaCl. The reaction mixture contained 0.25 mg/mL glycogen, 1 mM AMP, and 30 mM glucose 1-phosphate. The reaction was initiated by the addition of the enzyme to the reaction mixture.

Thermal Denaturation of UV-Irradiated Ph*b*. Thermal denaturation of UV-irradiated Ph*b* solutions was investigated by differential scanning calorimetry (DSC) using the DASM-4M adiabatic scanning microcalorimeter (Institute of Biological Instruments, Russian Academy of Sciences, Pushchino, Russia) with 0.47 mL capillary platinum cells. All measurements were taken in 0.08 M Hepes-NaOH buffer (pH 6.8) containing 0.1 M NaCl at a rate of heating of 1 °C/min using a temperature range of 20−85 °C and constant pressure of 2.2 atm. The dependence of the excess heat capacity versus temperature was calculated using Origin (MicroCal, Inc.).

Determination of the Refractive Index, Density, and Dynamic Viscosity. The values of the refractive index of 0.08 M Hepes-NaOH buffer (pH 6.8) containing 0.1 M NaCl and different concentrations of PEG-20000, TMAO, or Ficoll-70000 were determined in the IRF-22 refractometer. The density of 0.08 M Hepes-NaOH buffer (pH 6.8) containing 0.1 M NaCl and different concentrations of PEG-20000, TMAO, or Ficoll-70000 was determined in the DMA 4500 density meter (Anton Paar). The dynamic viscosity of 0.08 M Hepes-NaOH buffer (pH 6.8) containing 0.1 M NaCl in the presence of different concentrations of PEG-20000, TMAO, or Ficoll-70000 was determined in an automatic microviscosimeter (Anton Paar) in system 1.6/1.500 mm. The obtained values of refractive index, density, and dynamic viscosity are listed in Table S1 of the Supporting Information.

Dynamic Light Scattering (DLS). For light scattering measurements, a commercial Photocor Complex instrument (Photocor Instruments, Inc.) was used. A He−Ne laser (Coherent, model 31-2082, 632.8 nm, 10 mW) was used as a light source. The temperature of the sample cell was controlled by the proportional integral derivative temperature controller within ±0.1 °C. A quasi-cross correlation photon counting system with two photomultiplier tubes was used to increase the accuracy of particle sizing in the range from 0.5 nm to 5.0 μm. The scattering light was collected at a 90° scattering angle. The time of the accumulation of the autocorrelation function was 15 or 30 s. DynalS (Alango) was used for polydisperse analysis of DLS data.

The kinetics of aggregation of UV-irradiated Ph*b* was studied by DLS in 0.08 M Hepes-NaOH buffer (pH 6.8) containing 0.1 M NaCl. The buffer was placed in a cylindrical cell with an internal diameter of 6.3 mm and preincubated for 5 min at a given temperature (20 or 37 °C). Cells with a stopper were used to avoid evaporation. The aggregation process was initiated by the addition of an aliquot of UV-irradiated Ph*b* to the final volume of 0.5 mL. To study the effect of crowding on UV-irradiated Ph*b* aggregation, we preincubated a crowding agent (PEG-20000, Ficoll-70000, or TMAO) with buffer in the cell for 5 min before adding an aliquot of protein. All solutions were prepared with 0.08 M Hepes-NaOH buffer (pH 6.8) containing 0.1 M NaCl passed through a 20 nm "Anotop" filter (Whatman).

To calculate the initial rate of aggregation, we used the approaches we described previously.[51−54] The analysis of the literature data for the kinetics of protein aggregation showed that the dependence of the light scattering intensity (I) on time (t) followed the exponential law above the inflection point:

$$I = I_{lim}\{1 - \exp[-k_I(t - t^*)]\} \quad (1)$$

where I_{lim} is the limiting value of I at $t \to \infty$, k_I is the first-order rate constant, and t^* is a length on the abscissa axis cut off by the theoretical curve calculated from eq 1. The slope of a tangent to the theoretical curve passing through the point with coordinates $\{t = t^*; I = 0\}$ is equal to the product $k_I I_{lim}$. This product is a measure of the initial rate of aggregation.

Analytical Ultracentrifugation. Sedimentation velocity experiments were conducted at 20, 30, and 37 °C in a model E analytical ultracentrifuge (Beckman), equipped with absorbance optics, a photoelectric scanner, a monochromator, and a computer on-line. A four-hole rotor (An-F Ti) and 12 mm double sector cells were used. The rotor was preheated at 37 °C in the thermostat overnight before the run at 37 °C. The sedimentation profiles of UV-irradiated Ph*b* were recorded by measuring the absorbance at 280 nm. All cells were scanned simultaneously. The time interval between scans was 2.5 min. The sedimentation coefficients were estimated from the differential sedimentation coefficient distribution [ls-$g^*(s)$ vs s and $c(s)$ vs s] using SEDFIT.[55,56]

Size-Exclusion Chromatography. The mixture of α-crystallin and UV-irradiated Ph*b* was centrifuged at 14500*g* for 30 min using a MiniSpin+, Eppendorf centrifuge. The sediment was collected and washed twice using 40 mM sodium phosphate buffer (pH 6.8) containing 100 mM NaCl, 1 mM EDTA, and 3 mM NaN_3. The supernatant was loaded onto the column (Toyopearl TSK-gel HW-55 fine; 2.5 cm × 90 cm) and separated into the fractions at a flow rate of 1.3 mL/min (20 °C). Fractions of main peaks were collected for composition analysis by SDS−PAGE.

Sodium Dodecyl Sulfate−Polyacrylamide Gel Electrophoresis (SDS−PAGE). The polypeptide composition of fractions and sediment was analyzed by electrophoresis in 12.5% PAGE in the presence of SDS and dithiothreitol.[57] Sigma-Aldrich proteins α-lactalbumin (14.2 kDa), trypsin inhibitor (20.1 kDa), carbonic anhydrase (29 kDa), ovalbumin (45 kDa), and bovine serum albumin (66 kDa) were used as standards. The gels were stained with Coomassie R-250 and scanned with an Epson Perfection 4180 photoscanner.

Calculations. Origin 8.0 (OriginLab Corp.) and Scientist (MicroMath, Inc.) were used for the calculations. To characterize the degree of agreement between the experimental data and calculated values, we used the coefficient of determination R^2 (without considering the statistical weight of the measurements):[58]

$$R^2 = \frac{\sum_{i=1}^{i=n}(Y_i^{obs} - \bar{Y}^{obs})^2 - \sum_{i=1}^{i=n}(Y_i^{obs} - Y_i^{calc})^2}{\sum_{i=1}^{i=n}(Y_i^{obs} - \bar{Y}^{obs})^2} \quad (2)$$

where $\bar{Y}^{obs} = (1/n)(\sum_{i=1}^{i=n} Y_i)$ is the average of the experimental data (Y_i^{obs}), Y^{calc} is the theoretically calculated value of the function Y, and n is the number of measurements.

RESULTS

Effect of UV Irradiation on the Enzymatic Activity and Thermostability of Ph*b*. UV irradiation of Ph*b* solutions results in the loss of enzymatic activity. Figure 1 shows the

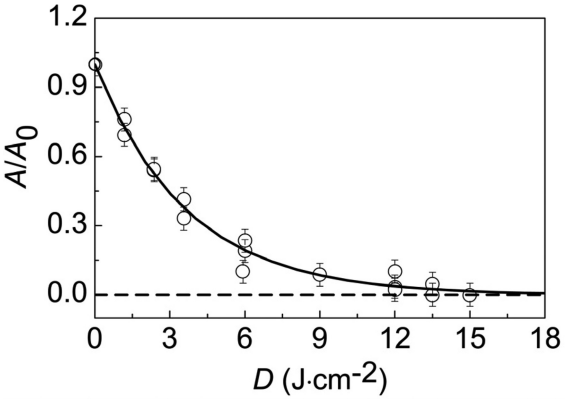

Figure 1. UV-induced inactivation of Ph*b* [80 mM Hepes buffer (pH 6.8) containing 0.1 M NaCl]. Dependence of the relative enzymatic activity A/A_0 (A_0 is the value of the enzymatic activity for nonirradiated Ph*b*) on UV dose (D). Points are experimental data. The solid curve was calculated from the exponential law $A/A_0 = \exp(-kD)$, where $k = \ln 2/D_{0.5}$.

dependence of the residual activity of Ph*b* on the UV dose. The inactivation process followed the exponential law, and the UV dose corresponding to 50% inactivation ($D_{0.5}$) was found to be 2.5 ± 0.1 J/cm^2.

UV-induced inactivation of Ph*b* is due to the disruption of the native structure of the protein globule. This conclusion was supported by the DSC measurements. Figure 2 shows the DSC

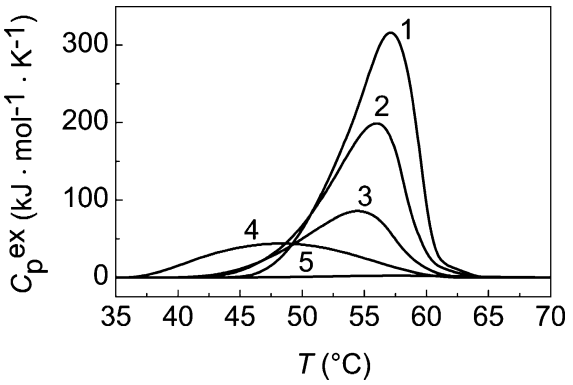

Figure 2. Thermostability of UV-irradiated Ph*b*. (A) Dependence of the excess heat capacity (C_p^{ex}) on temperature for nonirradiated Ph*b* (1) and Ph*b* irradiated by the following UV doses: 2.4 (2), 5.9 (3), 13.5 (4), and 27 J/cm^2 (5). The initial concentration of Ph*b* was 1.5 mg/mL. C_p^{ex} was calculated per Ph*b* dimer (M_r = 194800 Da).

profiles for the native and UV-irradiated Ph*b* samples. Thermal denaturation of Ph*b* is an irreversible process as evidenced by the fact that heat absorption is lacking upon repeated heating of the protein sample to 70 °C. The position of a maximum on the DSC profile (T_{max}) for native Ph*b* corresponds to 57.1 ± 0.1 °C. As one can see in Figure 2, UV irradiation of Ph*b* solutions results in the decrease in the area under the calorimetric curve, which is proportional to the amount of the native protein.

It should be noted that an increase in the UV dose is accompanied by the shift of the position of the maximum on the DSC profile toward the lower temperatures. The T_{max} values were found to be 56.0, 54.5, and 48.4 °C at UV doses of 2.4, 5.9, and 13.5 J/cm^2, respectively (curves 2–4, respectively, in Figure 2). At rather high UV doses, the full destruction of the native protein structure occurred (curve 5). The comparison of the DSC profiles for nonirradiated and irradiated proteins is essential for verification of the one-hit model, in which inactivation (denaturation) of the protein molecule proceeds on all-or-none principle as a result of absorption of one resulting photon.[59−61] If the one-hit model is operative, the position of T_{max} should remain the same in the course of irradiation. For Ph*b* irradiation, we observed a shift of the T_{max} position with an increase in the dose of radiation (Figure 2). It has been established that thermal denaturation of Ph*b* proceeds through the dissociative mechanism, and the diminution of the initial protein concentration in the denaturation experiments is accompanied by a shift of the maximal position on the DSC profile toward the lower temperatures for the reason that dilution provokes dissociation of Ph*b* dimers into more labile monomers.[62] However, such a shift in T_{max} is rather small. When the Ph*b* concentration decreases from 6.0 to 0.3 mg/mL, the change in T_{max} is 1.1 °C.[62] As one can see in Figure 2, the shift of the position of T_{max} at a UV dose of 13.5 J/cm^2 is 8.7 °C. Such a marked change in the T_{max} value means that a simple one-hit model is not valid. One can assume that UV irradiation results in the formation of less thermostable damaged protein molecules.

Characteristics of Protein Aggregates in the Solution of UV-Irradiated Ph*b*. DLS and sedimentation velocity analysis were used to characterize the protein aggregates formed in the solution of UV-irradiated Ph*b*. The conditions of irradiation were as follows: protein concentration of 1.5 mg/mL and UV radiation dose of 15 J/cm^2. The DLS experiments show that the native Ph*b* is characterized by a hydrodynamic radius of 5.31 ± 0.12 nm at 20 °C (Figure S1 of the Supporting Information). The polydispersity index (PI) for the particle size distribution calculated in accordance with the ISO standard[63] was found to be 0.049 ± 0.002. Such a low value of PI is typical of a monodisperse sample. The particles with an average hydrodynamic radius of 10.4 ± 0.2 nm and a higher PI value (0.30 ± 0.03) were registered in the solution of UV-irradiated Ph*b* [20 °C (Figure 3)]. The size of the protein aggregates

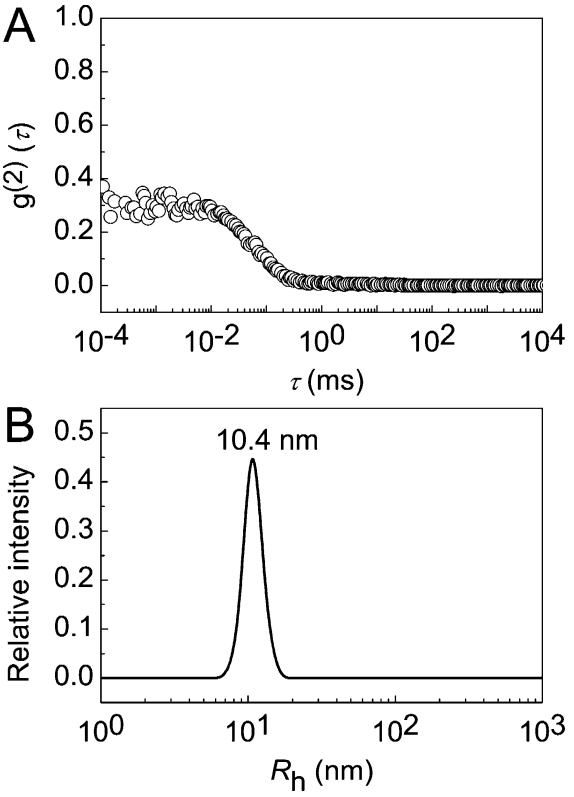

Figure 3. Characteristics of protein aggregates in a Ph*b* solution (1.5 mg/mL) irradiated with a UV dose of 15 J/cm^2. DLS measurements were taken at 20 °C: (A) autocorrelation function and (B) particle size distribution.

remained unchanged for at least 2 h at 20 °C. Thus, the essential part of UV-denatured Ph*b* aggregates with formation of small particles.

The sedimentation velocity data confirm the presence of aggregates in the solution of UV-irradiated Ph*b*. Analysis of the sedimentation profiles obtained for UV-irradiated Ph*b* [0.33 mg/mL (Figure 4A)] gives the differential sedimentation coefficient distribution ls-$g^*(s)$ presented in Figure 4B. As one can see, the distribution is rather wide, the weight-average sedimentation coefficient (s_{av}) being 20 S (standard deviation, σ, 8 S). One could expect that UV irradiation provokes not only denaturation but also dissociation of the dimeric form of the

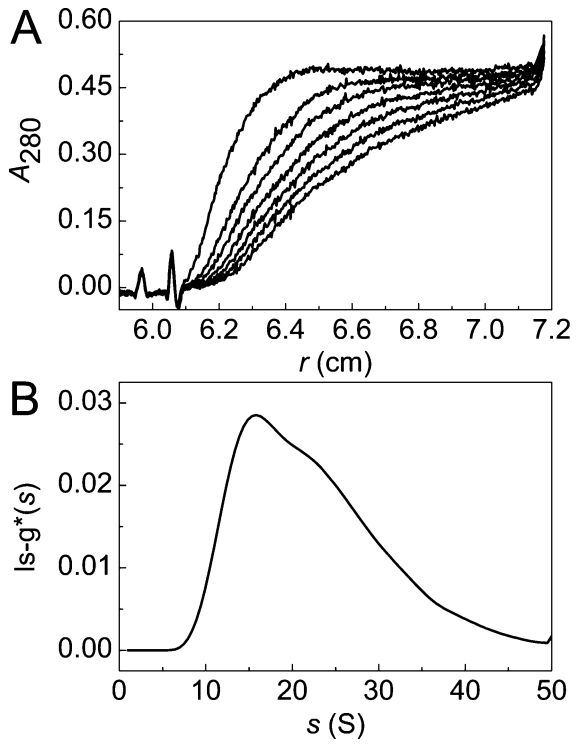

Figure 4. Sedimentation velocity analysis of UV-irradiated Ph*b* (0.33 mg/mL) at 22 °C. (A) Sedimentation profiles were registered at 280 nm with 2.5 min intervals. Selected profiles obtained with 5 min intervals are shown. The rotor speed was 40000 rpm. (B) Differential sedimentation coefficient distribution ls-$g^*(s)$ calculated from the data presented in panel A. The conditions of irradiation were as follows: initial Ph*b* concentration of 1.5 mg/mL and irradiation dose of 15 J/cm^2 (10 °C).

enzyme. However, there are no species corresponding to the monomeric form of Ph*b* (for which $s_{20,w}$ = 5.1 ± 0.1 S[64,65]) in the ls-$g^*(s)$ distribution. As for the dimeric form (native form for which $s_{20,w}$ = 8.6 S or denatured form), the portion of this form is negligibly small. When comparing the distribution patterns obtained from DLS or sedimentation velocity measurements, we should take into account the fact that DLS is characterized by a lower sensitivity than AUC.[66,67] This is why the particle size distribution presented in Figure 3 looks like a relatively homogeneous distribution. However, the PI value observed for UV-irradiated Ph*b* (0.3) indicates that the sample is polydisperse.

Effect of Crowding on Aggregation of UV-Irradiated Ph*b*. The protein aggregates formed in the course of UV irradiation are relatively stable at 20 °C. However, the markedly expressed aggregation is observed under crowding conditions. Addition of a crowding agent, PEG-20000, TMAO, or Ficoll-70000, stimulates the time-dependent increase in light scattering intensity (I) of UV-irradiated Ph*b* solutions (Figure 5A–C). The DLS measurements show that the increase in the I value is due to formation of large aggregates (Figure 5D–F). The hydrodynamic radii (R_h) of the protein aggregates reach values of ≥1000 nm.

Effect of Crowding on the Chaperone-like Activity of α-Crystallin. The elevation of the temperature results in the acceleration of aggregation of UV-irradiated Ph*b*. Figure 6A (curve 1) shows the kinetics of aggregation of the UV-irradiated protein (0.15 mg/mL) at 37 °C.

When studying the chaperone-like activity of α-crystallin, we observed that the protective effect of α-crystallin increases with an increasing chaperone concentration (Figure 6A). The smaller protein aggregates are formed in the presence of α-crystallin. This is illustrated in panels B and C of Figure 6, where the time-dependent increase in the hydrodynamic radius of the protein aggregates registered in the (B) absence or (C) presence of α-crystallin (0.15 mg/mL) is shown. It is worth noting that splitting of the particle population into two components

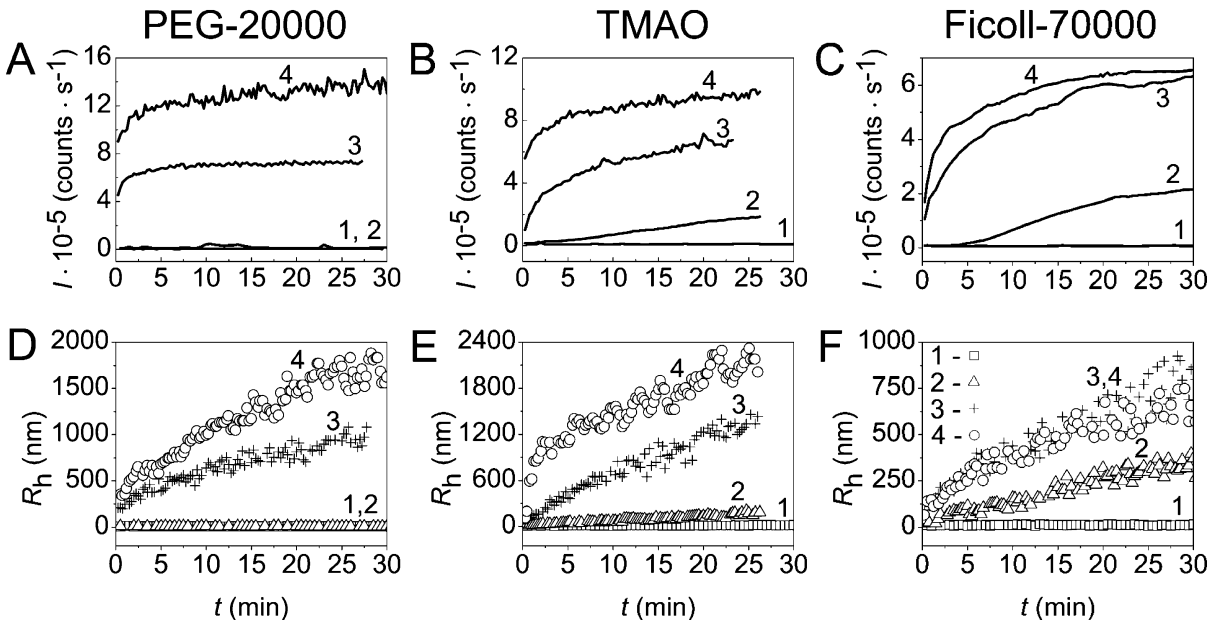

Figure 5. Effect of crowding agents on aggregation of UV-irradiated Ph*b* (0.3 mg/mL) at 20 °C. Dependences of light scattering intensity on time for PEG-20000 (A), TMAO (B), and Ficoll-70000 (C) and dependences of hydrodynamic radius of protein aggregates on time for PEG-20000 (D), TMAO (E), and Ficoll-70000 (F). Concentrations of PEG-20000 in panels A and D: 0 (1), 20 (2), 30 (3), and 40 mg/mL (4). Concentrations of TMAO in panels B and E: 0 (1), 0.5 (2), 0.75 (3), and 1 M (4). Concentrations of Ficoll-70000 in panels C and F: 0 (1), 100 (2), 125 (3), and 200 mg/mL (4). The conditions of irradiation were the same as those described in the legend of Figure 4.

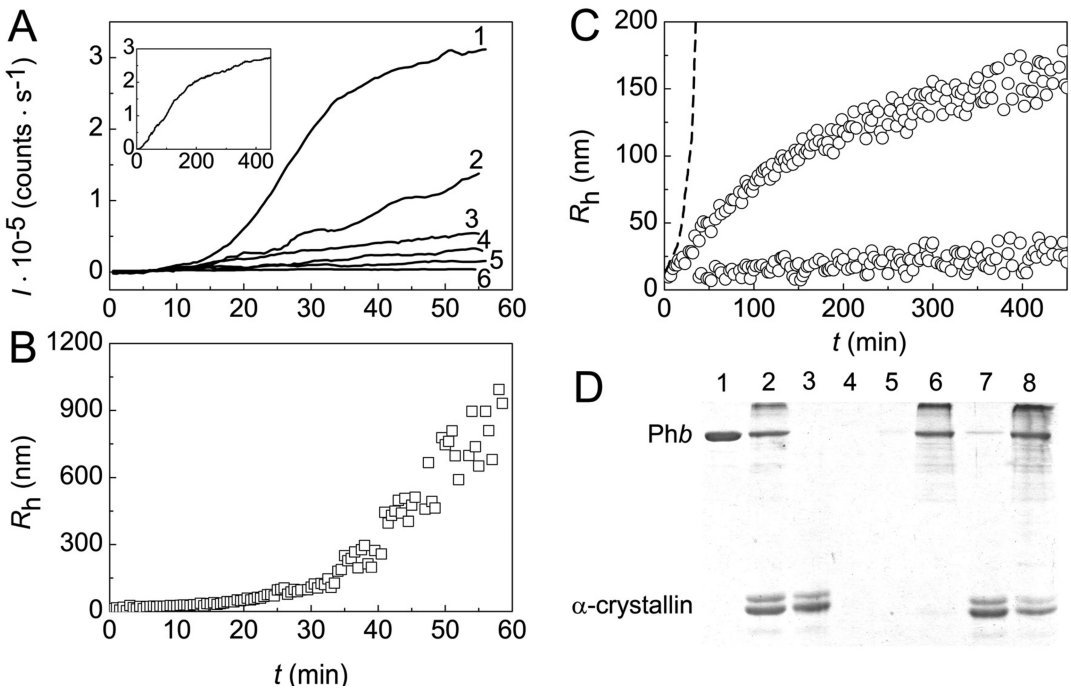

Figure 6. Protective effect of α-crystallin during aggregation of UV-irradiated Phb (0.15 mg/mL) at 37 °C. (A) Dependences of the light scattering intensity (I) on time obtained at 0 (1), 0.075 (2), 0.15 (3), 0.3 (4), and 1.0 mg/mL α-crystallin (5). Curve 6 corresponds to incubation of α-crystallin alone (1.0 mg/mL). The inset shows the dependence of I on time for aggregation of UV-irradiated Phb in the presence of α-crystallin at a concentration of 0.15 mg/mL. (B) Dependence of the hydrodynamic radius (R_h) of the protein aggregates on time obtained in the absence of α-crystallin. (C) Dependence of R_h of the protein aggregates on time obtained in the presence of 0.15 mg/mL α-crystallin. The dotted curve corresponds to the control obtained in the absence of α-crystallin. (D) SDS−PAGE analysis of protein substrate−chaperone interaction (12% PAGE): lane 1, native Phb; lane 2, UV-irradiated Phb/α-crystallin mixture; lanes 3 and 4, supernatant and sediment for preheated α-crystallin solution, respectively; lanes 5 and 6, supernatant and sediment for preheated UV-irradiated Phb solution, respectively; lanes 7 and 8, supernatant and sediment for preheated mixture of UV-irradiated Phb and α-crystallin, respectively. The samples were preheated for 5 h at 37 °C. Concentrations of UV-irradiated Phb and α-crystallin were identical (0.15 mg/mL). Sediments were separated by centrifugation at 20800*g*. The conditions of irradiation were the same as those described in the legend of Figure 4.

(two subpopulations) takes place when aggregation of UV-irradiated Phb is studied in the presence of α-crystallin (Figure 6C). This splitting becomes evident after 30 min. The R_h value for the smaller component increases from 12 to 25 nm in the time interval of 40−450 min, whereas the R_h value for the larger aggregates increases from 40 to 160 nm in the same time interval. The typical particle size distributions for aggregates of UV-irradiated Phb formed in the absence or presence of α-crystallin are shown in Figure S2 of the Supporting Information.

SDS−PAGE was used to analyze the composition of the aggregates of two types. When the time of incubation of the protein substrate/chaperone mixture at 37 °C was 5 h, rather large aggregates corresponding to the upper branch of $R_h(t)$ dependence were formed (see Figure 6C), and these aggregates may be separated by centrifugation. The supernatant obtained for the UV-irradiated Phb solution preheated in this manner contains negligible amounts of the protein (Figure 6D, lane 5), and almost all the protein precipitates (Figure 6D, lane 6). When heating α-crystallin, we do not observe this protein in the sediment (Figure 6D, lane 4). Lanes 7 and 8 correspond to the supernatant and the sediment for the preheated UV-irradiated Phb/α-crystallin mixture. As one can see in lane 8, the sediment contains, apart from UV-irradiated Phb, α-crystallin, suggesting that α-crystallin is incorporated into larger aggregates in the aggregate population.

To make a quantitative estimate of the chaperone-like activity of α-crystallin, we used a modified variant of eq 1:

$$I = I_0 + (I_{lim} - I_0)\{1 - \exp[-k_I(t - t^*)]\} \quad (3)$$

where I_0 is the initial value of the light scattering intensity (I) at time zero and t^* is a length on the $I = I_0$ horizontal line cut off by the theoretical curve calculated with eq 3. The slope of a tangent to the theoretical curve passing through the point with coordinates $\{t = t^*; I = I_0\}$ is equal to the product $k_I(I_{lim} - I_0)$, which is a measure of the initial rate of aggregation (v_{agg}). The principle of the method of calculation of v_{agg} is illustrated in Figure 7, where the dependence of the light scattering intensity on time for aggregation of UV-irradiated Phb (0.15 mg/mL) at 37 °C is shown ($I_0 = 0.196 \times 10^5$ counts/s). The fitting procedure gave the following values: $I_{lim} = (3.38 \pm 0.14) \times 10^5$ counts/s, $k_I = 0.100 \pm 0.003$ min^{-1}, and $t^* = 20.3 \pm 0.2$ min ($R^2 = 0.996$). The initial rate of aggregation ($v_{0,agg}$) was found to be $(2.98 \pm 0.04) \times 10^4$ counts s^{-1} min^{-1}. The addition of α-crystallin results in the diminution of the v_{agg} value. For example, at an α-crystallin concentration of 0.15 mg/mL (inset in Figure 6A), $v_{agg} = (0.256 \pm 0.013) \times 10^4$ counts s^{-1} min^{-1}. The $v_{agg}/v_{0,agg}$ ratio characterizes the chaperone-like activity of α-crystallin. When the α-crystallin concentration was 0.15 mg/mL, the $v_{agg}/v_{0,agg}$ ratio was found to be 0.086 ± 0.004 (Table 1). It should be noted that such a method of estimation of chaperone-like activity was used in refs 68−70.

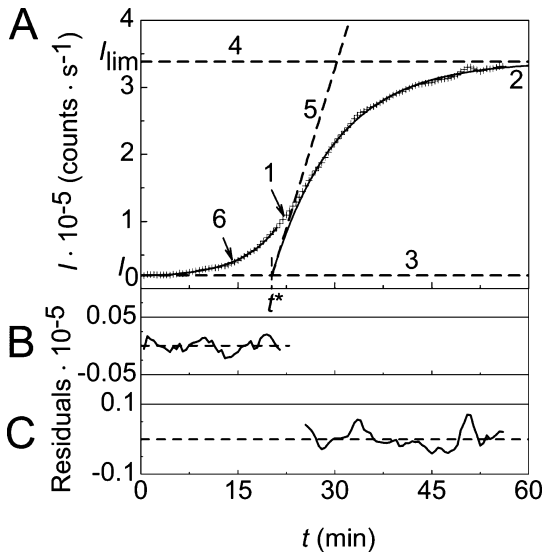

Figure 7. Quantitative estimation of chaperone-like activity. (A) Curve 1 is the experimental dependence of the light scattering intensity (I) on time obtained for aggregation of UV-irradiated Phb (0.15 mg/mL) at 37 °C. Curve 2 is the theoretical dependence of I on time corresponding to eq 3. Horizontal dotted line 3 is the initial value of I at $t = 0$ ($I = I_0$). Horizontal dotted line 4 is the limiting value of I at $t \rightarrow \infty$ ($I = I_{lim}$). Dotted line 5 is a tangent to curve 2 passing through the point with coordinates $\{t = t^*; I = I_0\}$; the slope of the tangent is equal to the product $k_i(I_{lim} - I_0)$. Theoretical curve 6 was calculated from eq 4 and used for description of the initial part of the dependence of I on time. Panels B and C are residual plots constructed for the demonstration of the applicability of eqs 4 and 3, respectively.

To analyze the initial part of the dependence of the light scattering intensity (I) on time (t), we used an empiric equation that is a stretched exponential function:

$$I = I_0 \exp\left[(\ln 2)\left(\frac{t}{t_{2I}}\right)^n\right] \quad (4)$$

where t_{2I} is the time at which $I = 2I_0$ and n is a constant. Solid curve 6 in Figure 7 was calculated from eq 4. The following values were found: $t_{2I} = 14.0 \pm 0.1$ min, and $n = 2.00 \pm 0.05$ ($R^2 = 0.998$).

The stretched exponential function was applied for description of the full kinetic curves of aggregation in refs 71−75. The following equation was used by these authors:

$$I = I_0 + (I_{lim} - I_0)\{1 - \exp[-(kt)^n]\} \quad (5)$$

where I_0 is the initial value of I at time zero, I_{lim} is the limiting value of I at $t \rightarrow \infty$, and k and n are constants. To describe the initial parts of the dependences of light scattering intensity on time for aggregation of UV-irradiated Phb, we propose to use a modified stretched exponential function represented by eq 4. It is interesting to note that according to our calculations the initial parts of the dependences of light scattering intensity on time for aggregation of UV-irradiated β_L-crystallin from eye lenses of steers at 37 °C[76] are satisfactorily described by eq 4. Thus, this equation may be useful for the analysis of the aggregation kinetics of UV-irradiated proteins.

It should be noted that eq 4 may be used for the description of the initial parts of the dependences of light scattering intensity on time obtained in the presence of α-crystallin. For example, when eq 4 was fit to the experimental data obtained for aggregation of UV-irradiated Phb at 0.075 mg/mL α-crystallin (curve 2 in Figure 6A), the following values were found: $t_{2I} = 18.8 \pm 0.5$ min, and $n = 1.04 \pm 0.02$ ($R^2 = 0.946$)

The method of estimation of the initial rate of aggregation described above was used to characterize the chaperone-like activity of α-crystallin under crowding conditions arising from the presence of PEG-20000 (Figure 8) and TMAO (Figure 9). Figure 8A demonstrates the acceleration of aggregation of UV-irradiated Phb at 37 °C in the presence of PEG-20000. The protective action of α-crystallin (0.15 mg/mL) was studied for aggregation of UV-irradiated Phb (0.15 mg/mL) in the presence of PEG-20000 at concentrations of 10 mg/mL (Figure 8B), 20 mg/mL (Figure 8C), and 30 mg/mL (Figure 8D). The values of the initial rate of aggregation calculated in the absence ($v_{0,agg}$) and presence of α-crystallin (v_{agg}) are listed in Table 1. The increase in the $v_{agg}/v_{0,agg}$ ratio with an increasing PEG-20000 concentration in the interval from 0 to 20 mg/mL (Table 1) means that the protective action of α-crystallin decreases with an increase in the concentration of the crowding agent. At a PEG-20000 concentration of 30 mg/mL, the $v_{agg}/v_{0,agg}$ value was 1.27 ± 0.11 (Table 1). Thus, there is a slight accelerating effect of α-crystallin at high PEG-20000 concentrations (Figure 8D).

Curves 2−4 in Figure 9 demonstrate the acceleration of aggregation of UV-irradiated Phb at 37 °C in the presence of TMAO (0.5−1.0 M). Curves 5−7 show the protective effect of α-crystallin (0.3 mg/mL), when the system contains the following concentrations of TMAO: 0 (1), 0.5 (2), 0.75 (3), and 1 M (4). As one can see, at rather high TMAO concentrations (1 M), the protective effect of α-crystallin is lacking. It should be noted that such a picture is retained even with a 10-fold increase in the α-crystallin concentration (data not shown).

When interpreting the data presented in Figure 9, we should take into account the results of the work by Lindner et al.[77] indicating that α-crystallin cannot interact efficiently with rapidly aggregating and precipitating proteins. Therefore, in strict terms, it is unclear whether the formation of a complex between α-crystallin and UV-irradiated Phb occurs at the initial stages of aggregation under crowding conditions. To gain better insight into the action of α-crystallin under crowding conditions, we performed experiments in which the crowding agent was added to the solution that contained previously formed complexes involving UV-irradiated Phb and α-crystallin.

Table 1. Effect of Crowding Arising from the Presence of PEG-20000 (30 mg/mL) on the Protective Action of α-Crystallin (0.15 mg/mL) during Aggregation of UV-Irradiated Phb (0.15 mg/mL) at 37 °C[a]

[PEG-20000] (mg/mL)	$v_{0,agg}$ (counts s^{-1} min^{-1})	v_{agg} (counts s^{-1} min^{-1})	$v_{agg}/v_{0,agg}$
0	$(2.98 \pm 0.04) \times 10^4$	$(0.256 \pm 0.013) \times 10^4$	0.086 ± 0.004
10	$(3.50 \pm 0.14) \times 10^4$	$(2.03 \pm 0.18) \times 10^4$	0.58 ± 0.07
20	$(5.27 \pm 0.19) \times 10^4$	$(3.87 \pm 0.16) \times 10^4$	0.73 ± 0.06
30	$(13.0 \pm 0.5) \times 10^4$	$(16.4 \pm 0.8) \times 10^4$	1.27 ± 0.11

[a] $v_{0,agg}$ and v_{agg} are the initial rates of aggregation in the absence and presence of α-crystallin, respectively.

dx.doi.org/10.1021/bi201030y | Biochemistry 2011, 50, 10607−10623

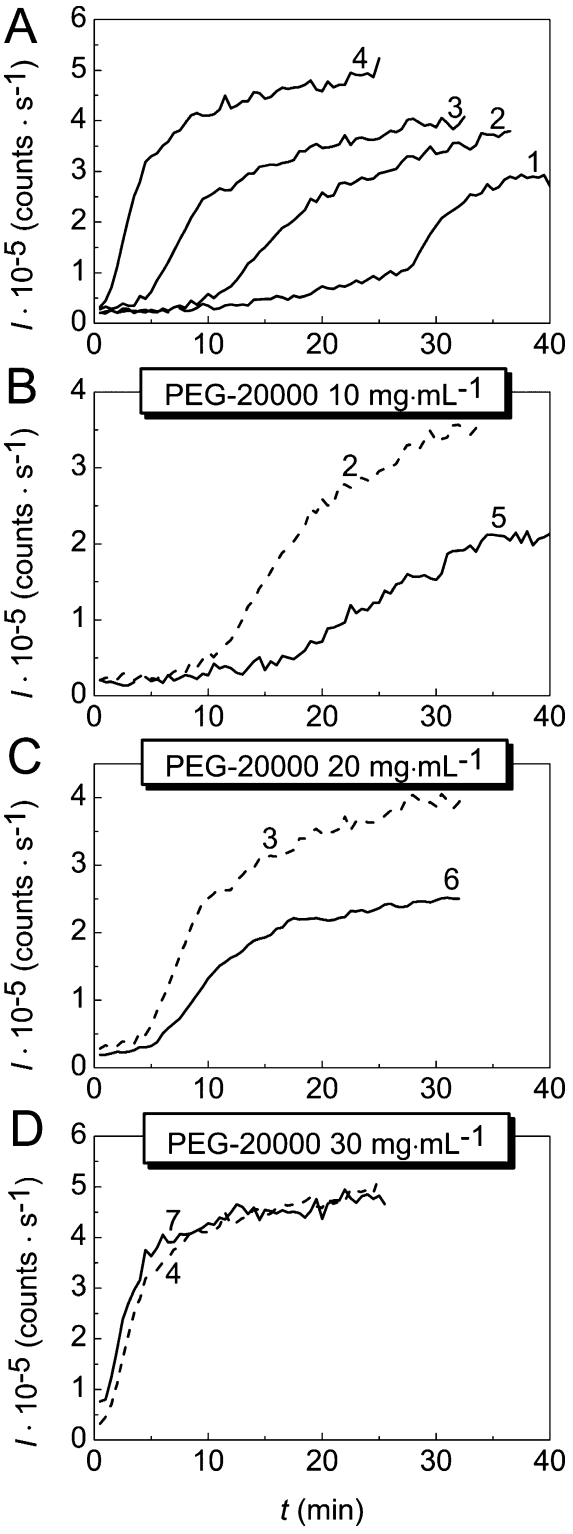

Figure 8. Effect of crowding arising from the presence of PEG-20000 on the chaperone-like activity of α-crystallin at 37 °C. (A) Dependences of light scattering intensity (I) on time for aggregation of UV-irradiated Ph*b* (0.15 mg/mL) in the absence of PEG-20000 (1) and in the presence of 10 (2), 20 (3), and 30 mg/mL PEG-20000 (4). (B–D) Chaperone-like activity of α-crystallin in the presence of 10, 20, and 30 mg/mL PEG-20000, respectively. Curves 5–7 correspond to aggregation of UV-irradiated Ph*b* in the presence of α-crystallin (0.15 mg/mL). The conditions of irradiation were the same as those described in the legend of Figure 4.

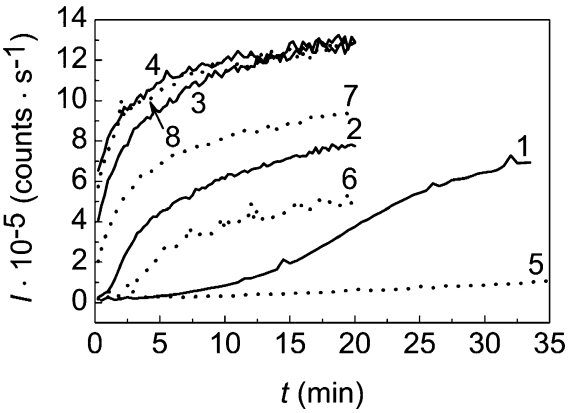

Figure 9. Effect of crowding arising from the presence of TMAO on the chaperone-like activity of α-crystallin at 37 °C. Dependences of light scattering intensity (I) on time for aggregation of UV-irradiated Ph*b* (0.3 mg/mL) in the absence of any additives (1) and in the presence of 0.5, 0.75, and 1 M TMAO (curves 2–4, respectively). Curves 5–8 correspond to aggregation of UV-irradiated Ph*b* registered in the presence of α-crystallin (0.3 mg/mL) and 0, 0.5, 0.75, and 1 M TMAO, respectively.

As one can see in Figure 10A, α-crystallin at a concentration of 1.5 mg/mL completely suppresses aggregation of UV-irradiated Ph*b* (0.3 mg/mL) at 37 °C (cf. curves 1 and 2). It should be noted that the aggregation process comes to a halt immediately after addition of α-crystallin. This fact suggests that mixing UV-irradiated Ph*b* and α-crystallin results in fast formation of the chaperone–substrate complex. The addition of the crowding agents with different chemical natures (PEG-20000, TMAO, and Ficoll-70000) induces well-defined aggregation of the protein substrate. Thus, α-crystallin losses its ability to prevent aggregation of a protein substrate under crowding conditions.

Calculations of the size of the particles in the system of UV-irradiated Ph*b*, α-crystallin, and a crowding agent showed that large aggregates ($R_h \approx 130–160$ nm) appeared immediately after addition of the crowding agent. Further sticking of these aggregates explains the observed increase in the light scattering intensity. A typical picture observed for PEG-20000 (30 mg/mL) is represented in Figure 10B. The population of the protein aggregates consists of two components. The size of the relatively small aggregates remains practically unchanged over time ($R_h \approx 12$ nm). The R_h value for larger aggregates reaches 640 nm within 3 min of the addition of PEG-20000. The additional data of this splitting of the aggregate population after the addition of the crowding agent are listed in Figures S3 and S4 of the Supporting Information

AUC Studies of Interaction between UV-Irradiated Ph*b* and α-Crystallin. Sedimentation velocity experiments allow detection of the changes in the oligomeric structure of α-crystallin upon exposure to elevated temperatures. These experiments are of special interest because it was shown that the chaperone-like activity of α-crystallin increased with an increase in temperature.[69,78–82] We studied the effect of crowding agents on the sedimentation behavior of α-crystallin at different temperatures. When the temperature was 25 or 30 °C, there were no significant changes in the differential sedimentation coefficient distribution $c(s)$ for α-crystallin under crowding conditions arising from the presence of TMAO or PEG-20000. As an example, Figure 11 shows the $c(s)$ distributions for α-crystallin (0.6 mg/mL) alone and for α-crystallin in the presence of 1 M TMAO or 20 mg/mL PEG-20000 at 30 °C. α-Crystallin is characterized by a broad $c(s)$

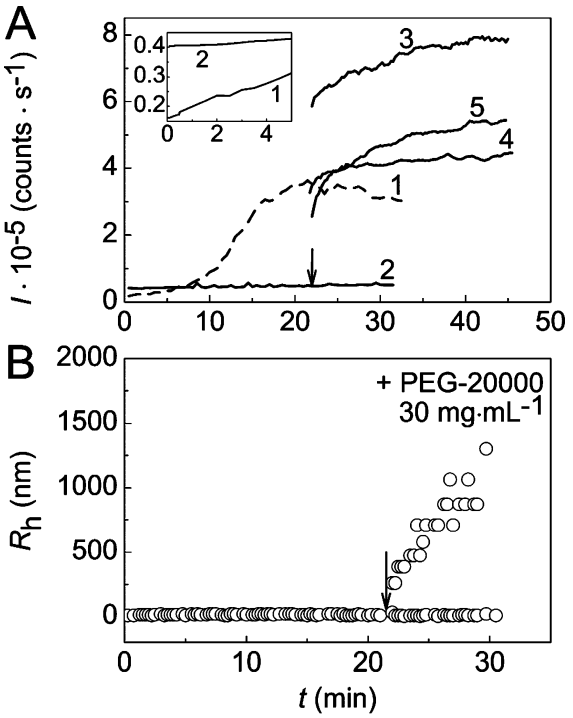

Figure 10. Decrease in the chaperone-like activity of α-crystallin under crowding conditions. (A) Dependence of light scattering intensity (I) on time for aggregation of UV-irradiated Phb (0.15 mg/mL) at 37 °C in the absence of any additives and in the presence of 1.5 mg/mL α-crystallin (curves 1 and 2, respectively). The inset in panel A shows the initial parts of curves 1 and 2 on an enlarged scale. Curves 3−5 correspond to aggregation of UV-irradiated Phb registered in the presence of α-crystallin (1.5 mg/mL) after the addition (final concentrations) of 30 mg/mL PEG-20000, 1 M TMAO, and 90 mg/mL Ficoll-70000, respectively. The arrow points to the moment of addition of the crowding agents. (B) Average values of the hydrodynamic radii of the particles registered in the mixture of UV-irradiated Phb (0.15 mg/mL) and α-crystallin (1.5 mg/mL) at 37 °C. The arrow points to the moment of addition of PEG-20000 at a final concentration of 30 mg/mL.

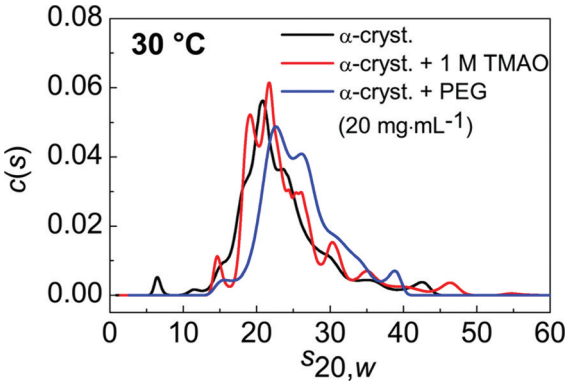

Figure 11. Sedimentation behavior of α-crystallin (0.6 mg/mL) in the absence and presence of crowding agents (1 M TMAO or 20 mg/mL PEG-20000) at 30 °C. The rotor speed was 34000 rpm. $c(s)$ sedimentation coefficient distributions obtained at 30 °C were transformed to standard $s_{20,w}$ distributions.

distribution with an s_{av} value of 22.9 S (σ = 6.5 S). Slightly enhanced values of s_{av} were obtained in the presence of 1 M TMAO (s_{av} = 23.8 S) or 20 mg/mL PEG-20000 (s_{av} = 25.7 S) (σ = 5.4 and 2.9 S, respectively). It should be noted that there is a small $s_{20,w}$ = 6.3 S peak in the $c(s)$ distribution of α-crystallin. This peak presumably corresponds to the dissociated forms of α-crystallin and disappears in the $c(s)$ distribution obtained for α-crystallin in the presence of the crowding agents. Heating of α-crystallin at 37 °C for 4 h in the absence or presence of TMAO or PEG-20000 results in some reduction in the s_{av} values (Figure 12). For α-crystallin alone, the s_{av} value was

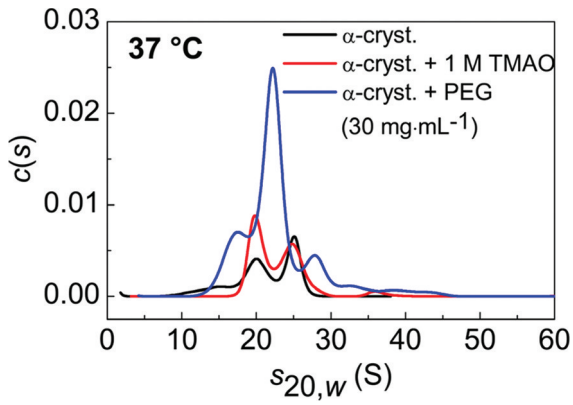

Figure 12. Sedimentation behavior of α-crystallin (0.17 mg/mL) in the absence and presence of crowding agents (1 M TMAO or 30 mg/mL PEG-20000) at 37 °C. Before centrifugation, samples were heated for 4 h at 37 °C. The rotor speed was 40000 rpm. $c(s)$ sedimentation coefficient distributions obtained at 37 °C were transformed to standard $s_{20,w}$ distributions.

found to be 21.1 S (σ = 5.5 S). The following values of s_{av} were obtained in the presence of 1 M TMAO or 30 mg/mL PEG-20000: 22.0 S (σ = 3.4 S) and 20.9 S (σ = 2.8 S), respectively. Increasing the time of incubation is accompanied by the appearance of the larger particles with higher sedimentation coefficients (Figure S5 of the Supporting Information).

The interaction of UV-irradiated Phb and α-crystallin was studied at 30 and 37 °C. In Figure 13A, the $c(s)$ distributions for UV-irradiated Phb (0.3 mg/mL), α-crystallin (0.6 mg/mL), and their mixture at 30 °C are compared. Before being run, the samples were incubated for 1 h at 30 °C. The shape of the $c(s)$ distribution for UV-irradiated Phb indicates that polydispersity becomes markedly higher than that observed at 20 °C (cf. Figure 4). This broadening of the $c(s)$ distribution is due to the acceleration of aggregation at 30 °C. The position of the main peak of α-crystallin in the $c(s)$ distribution for α-crystallin was found to be 21 S. The $c(s)$ distribution for the mixture of UV-irradiated Phb and α-crystallin includes, apart from the $s_{20,w}$ = 21 S peak, two peaks with lower $s_{20,w}$ values, namely, 6.2 and 10.5 S, suggesting that these peaks correspond to the complexes of the denatured Phb with the dissociated forms of α-crystallin.

Panels B and C of Figure 13 show the $c(s)$ distributions obtained for α-crystallin and its mixture with UV-irradiated Phb in the presence of 1 M TMAO or 20 mg/mL PEG-20000, respectively. The control $c(s)$ distributions for UV-irradiated Phb are lacking in these panels because the irradiated protein preincubated with 1 M TMAO or 20 mg/mL PEG-20000 for 1 h at 30 °C almost completely precipitated during rotor acceleration. The $c(s)$ distribution calculated for the mixture in the presence of 1 M TMAO includes $s_{20,w}$ = 8.0 and 11.5 S peaks. These peaks are lacking in the control $c(s)$ distribution for α-crystallin in the presence of 1 M TMAO. The $c(s)$ distribution for the mixture of UV-irradiated Phb and α-crystallin calculated in the presence of 20 mg/mL PEG-20000

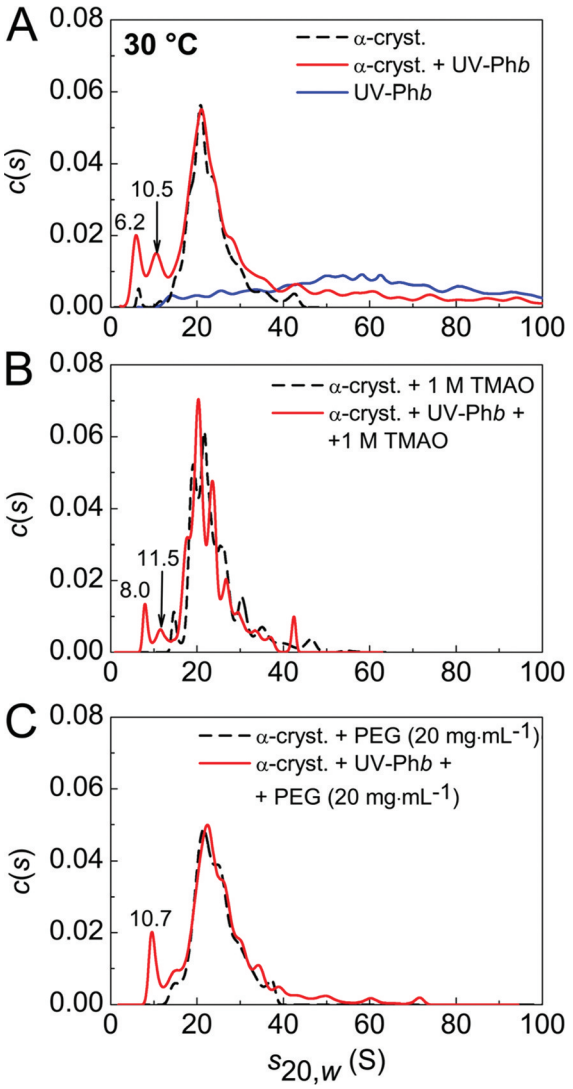

Figure 13. Effect of crowding on interaction of UV-irradiated Ph*b* with *α*-crystallin at 30 °C. (A) *c*(*s*) differential sedimentation coefficient distributions for UV-irradiated Ph*b*, *α*-crystallin, and their mixture. (B) *c*(*s*) distributions for *α*-crystallin and its mixture with UV-irradiated Ph*b* in the presence of 1 M TMAO. (C) *c*(*s*) distributions for *α*-crystallin and its mixture with UV-irradiated Ph*b* in the presence of 20 mg/mL PEG-20000. The concentrations of UV-irradiated Ph*b* and *α*-Crystallin were 0.3 and 0.6 mg/mL, respectively. Before being run, the samples were incubated for 1 h at 30 °C. The rotor speed was 34000 rpm. *c*(*s*) sedimentation coefficient distributions obtained at 30 °C were transformed to standard $s_{20,w}$ distributions.

includes the $s_{20,w}$ = 10.7 S peak, which is lacking in the control *c*(*s*) distribution of *α*-crystallin in the presence of PEG-20000. One can suppose that the $s_{20,w}$ < 15 S peaks correspond to the complexes of denatured Ph*b* with *α*-crystallin. The obtained results suggest that formation of a complex between UV-irradiated Ph*b* and *α*-crystallin occurs under crowding conditions.

The chaperone-like activity of *α*-crystallin under crowding conditions was studied by us at the physiological temperature of 37 °C (Figures 8 and 9). Therefore, it was of special interest to investigate the interaction of UV-irradiated Ph*b* and *α*-crystallin in the presence of crowding agents by analytical AUC at this temperature. In these experiments, we used a relatively high concentration of UV-irradiated Ph*b*, namely, 0.8 mg/mL. The concentration of *α*-crystallin was 0.17 mg/mL. The Ph*b* subunit:*α*-crystallin subunit molar ratio was 1:1, whereas the analogous value in the experiments conducted at 30 °C was 0.1:1. The higher concentration of UV-irradiated Ph*b* was used to provide the higher degree of saturation of *α*-crystallin by the protein substrate.

The samples of UV-irradiated Ph*b* were incubated for 4 h at 37 °C in the absence or presence of crowding agents. After such a treatment, the irradiated protein precipitated during acceleration of the rotor. Therefore, the control *c*(*s*) distribution for UV-irradiated Ph*b* is lacking in Figure 14, where the *c*(*s*) distributions for *α*-crystallin and its mixture with UV-irradiated Ph*b* heated for 4 h at 37 °C in the absence and presence of crowding agents are represented. The *c*(*s*) distribution for *α*-crystallin includes (Figure 14A) the $s_{20,w}$ = 20 and 25.1 S peaks. There are four distinct peaks for the mixture: $s_{20,w}$ = 9.6, 18.1, 21.0, and 26.0 S. From comparison of the *c*(*s*) distributions for *α*-crystallin and its mixture with UV-irradiated Ph*b*, one may conclude that the peaks in the *c*(*s*) distribution for the mixture correspond mainly to the complexes of *α*-crystallin with the protein substrate. It is likely that the $s_{20,w}$ = 9.6 S peak is indicative of the existence of the complex formed by the denatured protein substrate with the dissociated species of *α*-crystallin. It is not improbable that $s_{20,w}$ = 18.1 and 21.0 peaks contain, apart from the UV-irradiated Ph*b*–*α*-crystallin complex, small amounts of nonbound *α*-crystallin.

Figure 14 (panels B and C) shows the sedimentation behavior of *α*-crystallin and its mixture with UV-irradiated Ph*b* heated for 4 h at 37 °C in the presence of crowding agents. The *c*(*s*) distributions for *α*-crystallin in the presence of 1 M TMAO include the $s_{20,w}$ = 19.8 and 24.8 S peaks (Figure 14B). One can assume that the $s_{20,w}$ = 10.1, 15.7, 21.1, and 35.0 S peaks in the *c*(*s*) distributions for the mixture of UV-irradiated Ph*b* with *α*-crystallin in the presence of 1 M TMAO correspond mainly to complexes of *α*-crystallin and the protein substrate. The $s_{20,w}$ = 10.1 S peak probably points to the existence of the complex of the denatured substrate with the dissociated forms of *α*-crystallin. The complexes of such a type are formed under crowding conditions arising from the presence of PEG-20000 at a concentration of 30 mg/mL as evidenced by the appearance of $s_{20,w}$ = 8.9 and 13.7 S peaks in the *c*(*s*) distribution obtained for the mixture of UV-irradiated Ph*b* and *α*-crystallin (Figure 14C). Thus, the complexes of the denatured protein substrate with the dissociated species of *α*-crystallin are retained after incubation of the chaperone/substrate mixture for 4 h.

Study of Interaction of UV-Irradiated Ph*b* and *α*-Crystallin by SEC. Figure 15A shows SEC profiles for the mixture of intact Ph*b* and *α*-crystallin (profile with labels Ph*b* and *α*-cryst.) and the mixture of UV-irradiated Ph*b* and *α*-crystallin heated for 1 h at 37 °C (profile 1). The main peak (1b) of profile 1 corresponds to free *α*-crystallin, as evidenced by the SDS–PAGE data (Figure 15B, lane 5). Judging from the SDS–PAGE data, peaks $1a_1$, $1a_2$, and 1c correspond to the complexes of UV-irradiated Ph*b* with *α*-crystallin (lanes 7, 6, and 4 of Figure 15B, respectively). SEC profile 2 was obtained for the mixture of UV-irradiated Ph*b* and *α*-crystallin heated at 37 °C for 20 min in the absence of TMAO and thereafter for 10 min in the presence of 1 M TMAO. As in the case of profile 1, the main peak (2b) corresponds to free *α*-crystallin. This is evidenced by SDS–PAGE data (Figure 15B, lane 9). Only UV-irradiated Ph*b*–*α*-crystallin complexes smaller than intact *α*-crystallin are registered in this case (Figure 15A, peak 2a). SDS–PAGE data (Figure 15B, lane 10) support the fact that both proteins are incorporated in these complexes. SDS–PAGE

dx.doi.org/10.1021/bi201030y | *Biochemistry* 2011, 50, 10607–10623

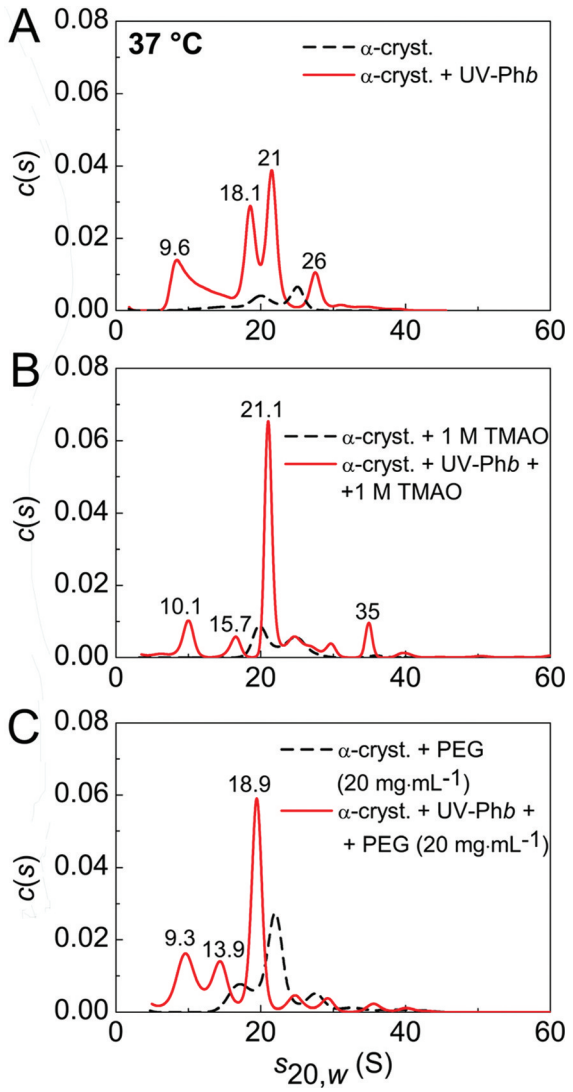

Figure 14. Effect of crowding on the interaction of UV-irradiated Ph*b* with *α*-crystallin at 37 °C. (A) *c*(*s*) differential sedimentation coefficient distributions for UV-irradiated Ph*b*, *α*-crystallin, and their mixture. (B) *c*(*s*) distributions for *α*-crystallin and its mixture with UV-irradiated Ph*b* in the presence of 1 M TMAO. (C) *c*(*s*) distributions for *α*-crystallin and its mixture with UV-irradiated Ph*b* in the presence of 30 mg/mL PEG-20000. The concentrations of UV-irradiated Ph*b* and *α*-crystallin were 0.8 and 0.17 mg/mL, respectively. Before being run, the samples were incubated for 4 h at 30 °C. The rotor speed was 40000 rpm. *c*(*s*) sedimentation coefficient distributions obtained at 37 °C were transformed to standard $s_{20,w}$ distributions.

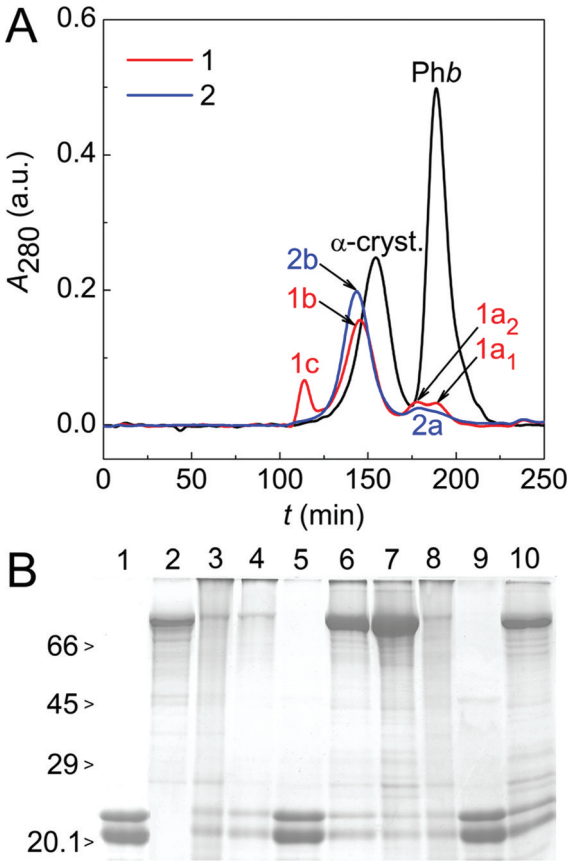

Figure 15. Interaction of UV-irradiated Ph*b* and *α*-crystallin studied by SEC and SDS–PAGE. (A) SEC (Toyopearl TSK-gel HW-55 fine column, 2.5 cm × 90 cm) of the mixtures of *α*-crystallin and UV-irradiated Ph*b*. For SEC profile 1, the mixture of UV-irradiated Ph*b* (1 mg/mL) and *α*-crystallin (1 mg/mL) with a volume of 6 mL was heated for 1 h at 37 °C. Upon separation of the sediment by centrifugation, the supernatant was loaded onto the column. For SEC profile 2, the mixture of UV-irradiated Ph*b* (1 mg/mL) and *α*-crystallin (1 mg/mL) with a volume of 6 mL was heated for 20 min at 37 °C. Then TMAO was added to the mixture (the final concentration of TMAO was 1 M). After incubation for 10 min at 37 °C, the sediment was separated by centrifugation and the supernatant was loaded onto the column. The peaks labeled Ph*b* and *α*-cryst. correspond to Ph*b* and *α*-crystallin, respectively, and were obtained for the mixture of intact Ph*b* (6 mg) and *α*-crystallin (7.3 mg). (B) SDS–PAGE of UV-irradiated Ph*b*, *α*-crystallin, and their mixtures: lane 1, *α*-crystallin; lane 2, native Ph*b*; lanes 3 and 8, sediments obtained under the conditions corresponding to SEC profiles 1 and 2, respectively; lanes 4–7, peaks 1c, 1b, $1a_2$, and $1a_1$, respectively; lanes 9 and 10, peaks 2b and 2a, respectively. Relative molecular masses (in kilodaltons) of standard proteins are indicated to the left of lane 1.

analysis of the sediments obtained on heating of the mixture of chaperone and protein substrate in the absence or presence of the crowding agent shows that in both cases the precipitate contains not only UV-irradiated Ph*b* but also *α*-crystallin (Figure 15B, lanes 3 and 8). These data indicate that interaction between UV-irradiated Phb and *α*-crystallin may result in the formation of insoluble aggregates containing both proteins.

DISCUSSION

First, we compared the test systems on the basis of thermal aggregation of nonirradiated and UV-irradiated proteins. The general process of thermal aggregation of nonirradiated protein involves a stage of unfolding of the protein molecule and the stages of aggregation of the denatured protein. In the modern view, the initial stage of aggregation is the formation of nuclei.[12,83] The theoretical analysis conducted by Ferrone[84] showed that for nucleation-dependent aggregation the accumulation of monomers incorporated into the aggregate proceeded according to the time-squared law. When studying the kinetics of thermal aggregation of proteins by DLS, we observed that at the moment when the initial increment in the light scattering intensity is observed, protein aggregates containing hundreds of denatured protein molecules are registered.[39,40,85−95] These primary aggregates were called the start aggregates. We could not detect intermediate states between the nonaggregated form of the protein and start aggregates. Thus, we inferred that the formation of the start

dx.doi.org/10.1021/bi201030y | *Biochemistry* 2011, 50, 10607–10623

aggregates proceeded on the all-or-none principle. On the basis of these experimental data, a model of protein aggregation was proposed according to which nuclei assemble rather quickly into start aggregates and further growth of aggregates is due to sticking of the start aggregates and higher-order aggregates.[39,85,90,96] For thermal aggregation of Phb [0.08 M Hepes buffer (pH 6.8) containing 0.1 M NaCl], the start aggregates with an R_h of 100 ± 1 nm were registered at 37 °C.[85] The aggregation process under discussion is depicted in Scheme 1. The fact that the initial stages of the general process

Scheme 1

Native protein → Unfolded protein → Nucleus → Start aggregates → Amorphous aggregates of higher order

of aggregation involve the stages of protein unfolding and stages of nucleation and formation of the start aggregates explains the appearance of a lag period on the kinetic curves of aggregation. To analyze the initial parts of the dependences of light scattering intensity (I):[97]

$$I = K_{agg}(t - t_0)^2 \quad (t > t_0) \tag{6}$$

In this equation, t_0 is a point in time at which the light scattering intensity begins to increase and K_{agg} is a constant that may be used as a measure of the initial rate of aggregation. Parameter t_0 corresponds to the moment of the origination of the start aggregates. The applicability of eq 6 was demonstrated for thermal aggregation of Phb,[91,97,98] glyceraldehyde-3-phosphate dehydrogenase (GAPDH),[93] and creatine kinase from rabbit skeletal muscle.[94]

The testing procedure for the agents that are able to exert an influence on the stages of protein aggregation with the aid of the test system based on thermal protein aggregation has the following disadvantages. The agents being tested may affect not only the stages of protein aggregation but also the stages of unfolding of the protein molecule. For example, when studying suppression of thermal aggregation of GAPDH and Phb from rabbit skeletal muscle by α-crystallin, we observed that α-crystallin has a destabilizing effect on the protein molecules because of the interaction with early intermediates of protein unfolding.[65,88,99,100]

The study of the effects of the crowding agents on protein aggregation with the aid of the test systems based on thermal aggregation of a protein substrate is also complicated by the fact that crowding exerts an influence on the stage of protein unfolding. In general, one can expect that effects of crowding on the stages of protein unfolding and protein aggregation will be oppositely directed.

The merit of a test system based on aggregation of UV-irradiated proteins is the possibility of testing different agents (including crowding agents) that directly affect the stage of aggregation of the protein molecules. UV irradiation results in denaturation of a protein substrate followed by assembly of denatured molecules into primary aggregates. In the case of UV-irradiated Phb, the hydrodynamic radius of the primary aggregates was found to be 10.4 ± 0.2 nm. In an earlier article,[76] we showed that a solution of UV-irradiated β_L-crystallin from eye lenses of steers contained primary aggregates with hydrodynamic radii of 20−24 nm. Primary aggregates are relatively stable at room temperature; however, they reveal a marked propensity to aggregate further at 37 °C. Thus, thermal aggregation of the UV-irradiated protein substrate follows the simple mechanism depicted in Scheme 2. This scheme does not

Scheme 2

Primary aggregates → Aggregates of higher order

contain the nucleation stage and the stage of assembly of nuclei into primary aggregates. It should be noted that for both test systems the aggregation process starts with an acceleration demonstrated by the light scattering intensity versus time plots. However, there is an essential difference between the kinetic curves of aggregation obtained for these test systems. In the case of a test system based on thermal aggregation of the nonirradiated protein substrate, the initial increment of the light scattering intensity is registered at the definite point in time t_0 ($t_0 \neq 0$; see eq 6). As for the test system based on aggregation of the UV-irradiated protein substrate, the initial parts of the dependences of light scattering intensity on time are described by eq 4, which does not contain parameter t_0. This means that the increase in the light scattering intensity is registered immediately at $t > 0$. Such peculiarities of the aggregation kinetics of UV-irradiated protein are due to the fact that the nucleation stage and the stage of formation of primary aggregates had been completed by the time of completion of the UV irradiation pretreatment. It is clear that this test system does not allow us to study the effects of different factors on the initial stages of aggregation (nucleation and formation of primary clusters).

In this work, using the test system based on aggregation of UV-irradiated Phb, we showed that crowding agents (PEG-20000, Ficoll-70000, and TMAO) stimulated aggregation of the protein substrate. It should be noted that under selected experimental conditions (20 °C) UV-irradiated Phb was relatively stable in the absence of a crowding agent. Acceleration of the aggregation process was observed in the presence of crowding agents that had different chemical natures. Thus, such an accelerating action of the crowding agent is mainly due to excluded-volume effects in qualitative accord with crowding theory.[7] It is significant that the used system allows registration of the effects of crowding just on the aggregation stage, namely the aggregation stage depicted in Scheme 2. When working with the test system based on aggregation of the UV-irradiated protein substrate, we should take into account the fact that after the completion of the UV irradiation procedure the protein solution does not contain denatured protein molecules in a nonaggregated form, because they have been assembled into primary clusters. A priori, one could not predict the effect of α-crystallin on further sticking of primary clusters. This work is the first to demonstrate the antiaggregation ability of α-crystallin with respect to the UV-irradiated protein substrate. The practically complete suppression of UV-irradiated Phb aggregation was observed at rather high concentrations of α-crystallin (curve 5 of Figure 6A).

The distinctive property of aggregation of UV-irradiated Phb in the presence of α-crystallin is the splitting of the aggregate population into two components (subpopulations) that aggregate with different rates (Figure 6C). Such a splitting of the aggregate population was first discovered by Khanova et al.,[39] who studied the kinetics of thermal aggregation of β_L-crystallin in the presence of α-crystallin. These authors suggested that two kinds of complexes were formed in the

β_L-crystallin/α-crystallin system. The complexes of the first kind are characterized by a relatively low density of aggregation sites on the particle surface and therefore reveal a weak propensity to aggregate. On the other hand, the complexes of the second kind are characterized by a relatively high density of aggregation sites on the particle surface. Because of this, each collision of the interacting particles results in their sticking. In other words, the aggregation process of such a type proceeds in the diffusion-limited regime (so-called diffusion-limited cluster–cluster aggregation[101]). Similar splitting of the aggregate population into two components was also observed for thermal aggregation of rabbit muscle GAPDH[95,96] and aspartate aminotransferase from pig heart mitochondria[89] in the presence of α-crystallin.

On the basis of the data for the kinetics of aggregation of UV-irradiated Ph*b* in the presence of α-crystallin (Figure 6) and the results of sedimentation velocity and SEC analysis of the mixtures of UV-irradiated Ph*b* and α-crystallin incubated at 30 or 37 °C for a definite period of time (Figures 13A, 14A, and 15), we propose the following scheme of interaction of the chaperone with the protein substrate (Scheme 3). We assume

Scheme 3

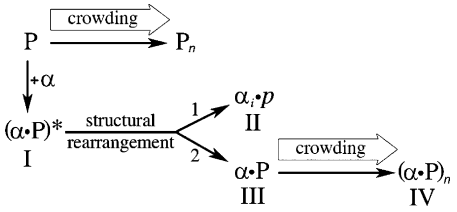

that the addition of α-crystallin (α) to the protein substrate (UV-irradiated Ph*b*; P) results in the relatively fast formation of the (α·P)* complex (complex I). It is well-known that the quaternary structure of α-crystallin is highly dynamic, with subunits capable of freely and rapidly exchanging between oligomers.[48,102−107] Because of the high mobility of α-crystallin, particle complex I is very unstable and undergoes structural rearrangement that ultimately results in the formation of a complex containing dissociated forms of α-crystallin, α_i, and dissociated forms of protein substrate, *p* (this complex, α_i·*p*, is designated as complex II), and water-soluble α-crystallin-unfolded target protein high-molecular weight complex α·P (complex III). The rearrangement of the (α·P)* complex may involve the following stages: splitting out of the α-crystallin subunit from the oligomer, disassembly of the protein substrate (primary aggregates of UV-irradiated Ph*b*, P) as a result of interaction with the α-crystallin matrix, binding of the protein substrate to the dissociated forms of α-crystallin, and reassociation of α_i·*p* particles into high-molecular weight complexes containing entrapped substrate (α·P, complex III).

The idea of forming a complex between dissociated forms of α-crystallin and a protein substrate followed by the assembly of these complexes into high-molecular weight particles was developed by Carver and co-workers[108,109] (see also refs 106 and 110). When using GAPDH and Ph*b* as protein substrates, we elucidated the formation of complexes between a target substrate and dissociated forms of α-crystallin at elevated temperatures (45 and 48 °C, respectively).[88,95,100] It is suggested that the products of dissociation of GAPDH and Ph*b* oligomers are incorporated in the target protein–α-crystallin complexes, α_i·*p*. It should be noted that according to the current view dissociation of small heat shock proteins is required for recognition and binding of structurally unstable proteins.[110−116]

Consider the SEC and AUC data as well as the electrophoresis data in the frame of the proposed Scheme 3. The SEC profile for the UV-irradiated Ph*b*/α-crystallin mixture, apart from α-crystallin (peak 1b in Figure 15), contains two peaks that were identified by us as protein substrate–α-crystallin complexes. The peaks with masses lower than that of α-crystallin (peaks $1a_1$ and $1a_2$) correspond to the α_i·*p* complex, i.e., complex II in Scheme 3, whereas the peak with a mass larger than that of α-crystallin (peak 1c) corresponds to the soluble protein substrate–α-crystallin high-molecular weight complex α·P (complex III). In the $c(s)$ sedimentation coefficient distributions, complex II manifests itself as species with $s_{20,w}$ = 6.2 and 10.5 S peaks (Figure 13A, 30 °C) and an $s_{20,w}$ = 9.6 S peak (Figure 14A, 37 °C). In Figure 13A, the Ph*b* subunit:α-crystallin subunit molar ratio was 0.1:1. At this molar ratio, nonbound α-crystallin is revealed as a main $s_{20,w}$ = 21.0 S peak (Figure 13A). At higher temperature (37 °C) and a higher UV-irradiated Ph*b* concentration (1:1 molar ratio), the $c(s)$ distribution contains several peaks ($s_{20,w}$ = 18.1, 21.0, and 26.0 S) corresponding to target protein–α-crystallin complexes. Thus, complex III may exist as a polydisperse ensemble of structures. This is consistent with the recent results of Stengel et al.,[117] who have come to the conclusion that target protein–chaperone interaction results in the appearance of the polydisperse ensemble of complexes containing variable numbers of both chaperone and target protein molecules. The splitting of the aggregation population into two subpopulations registered for aggregation of UV-irradiated Ph*b* in the presence of α-crystallin (Figure 6C) may be interpreted as follows. The subpopulation consisting of smaller particles is a mixture of unbound α-crystallin and complexes II and III. Complex II (α_i·*p*) is rather stable and reveals a weak propensity to aggregate. As for complex III (α·P), this complex is prone to aggregation, and its aggregation explains the appearance of the large aggregates, the size of the latter monotonously increasing over time [the upper branch of the $R_h(t)$ dependence represented in Figure 6C]. Precipitation of such aggregates takes place when the R_h values reach several micrometers. Complex $(\alpha·P)_n$ (complex IV) in Scheme 3 refers to precipitating aggregates.

Taking into account Scheme 3, we can postulate the existence of two types of chaperone-like activity. One of these types of chaperone-like activity is connected with the formation of relatively stable α_i·*p* complexes (pathway 1), whereas the other (pathway 2) is realized through the formation of α·P complexes that reveal a propensity to aggregate weaker than that of the original protein substrate. When crowding effects are discussed, these views of two types of chaperone-like activity are of utmost importance. Comparison of SEC profiles 1 and 2 in Figure 15 and analysis of the $c(s)$ distributions obtained under crowding conditions (Figures 13B,C and 14B,C) show that complex II remains in the nonaggregated state in the presence of crowding agents. On the other hand, crowding significantly facilitates aggregation of complex III, resulting in the formation of insoluble particles (complex IV). The electrophoresis data testify that inclusion of α-crystallin in the precipitate occurs (Figures 6D and 15B). The sharp increase in the light scattering intensity in the UV-irradiated Ph*b*/α-crystallin system after the addition of a crowding agent (Figure 10A) is due to aggregation of complex III. It becomes evident that the disappearance of the chaperone-like activity under crowding conditions

(Figures 8 and 9; see also refs 42 and 43) may be simply explained by the acceleration of aggregation of α·P complexes. Such a picture is observed only when the antiaggregation activity of α-crystallin is studied by measuring the light scattering intensity. However, the type of chaperone-like activity mentioned above is connected only with formation of α·P complexes (pathway 2). As for the type of chaperone-like activity that is connected to the formation of $\alpha_i{\cdot}p$ complexes (pathway 1), the activity of this type remains practically unchanged under crowding conditions.

The participation of sHsps in the formation of insoluble protein complexes has been discussed by several authors.[116,118] It is probable that the biochemical properties of insoluble protein complexes containing sHsp dramatically differ from those for the protein aggregates formed in the absence of sHsp in their toxicity, susceptibility to proteolytic degradation, and possibility of further refolding with participation of proper chaperones (Hsp100, Hsp40, and Hsp70).

In this work, we showed that the interaction of UV-irradiated Phb and α-crystallin was accompanied by the formation of two types of target protein−chaperone complexes: one type with a high rate of aggregation under crowding conditions and another type with a weak propensity to aggregate. The effect of crowding on structural rearrangement of the target protein−α-crystallin complex calls for further investigation. It is of special interest to study the formation of complexes between the dissociated form of sHsps and target protein under the conditions mimicking the crowded cell-like environment. Chebotareva et al.[119] were the first to discover the formation of the complexes of such a type in crowded media. They studied the interaction of Hsp27 with native phosphorylase kinase from rabbit skeletal muscle (PhK), which can be considered as a model target protein, under crowding conditions. Crowding provokes the formation of large aggregates of both Hsp27 and PhK. However, interaction of Hsp27 and PhK results in dissociation of large homo-oligomers of each protein with formation of small Hsp27·PhK complexes.

■ ASSOCIATED CONTENT

Supporting Information

Values of refractive index, density, and dynamic viscosity of solutions of PEG-20000, Ficoll-70000, and TMAO at 20 °C (Table S1); characterization of native Phb by DLS measurements at 20 °C (Figure S1); particle size distributions registered for UV-irradiated Phb (0.15 mg/mL) heated at 37 °C for 35 min in the absence of α-crystallin and for 400 min in the presence of α-crystallin (0.15 mg/mL) (Figure S2); particle size distributions registered at 37 °C for the mixture of UV-irradiated Phb (0.15 mg/mL) and α-crystallin (1.5 mg/mL) before the addition of PEG-20000 and within 3 min of the addition of PEG-20000 at a final concentration of 30 mg/mL (Figure S3); PEG-induced aggregation of Phb in the mixture of UV-irradiated Phb (0.15 mg/mL) and α-crystallin (1.5 mg/mL) at 35 °C registered by DLS (Figure S4); and sedimentation behavior of α-crystallin (0.2 mg/mL) in the absence and presence of crowding agents (1 M TMAO or 30 mg/mL PEG-20000) at 37 °C (Figure S5). This material is available free of charge via the Internet at http://pubs.acs.org.

■ AUTHOR INFORMATION

Corresponding Author

*Phone: +7 495 9525641. Fax: +7 495 9542732. E-mail: svetabaj@gmail.com (S.G.R.) or chebotareva@inbi.ras.ru (N.A.C.).

Funding

This study was funded by the Russian Foundation for Basic Research (Grants 11-04-01271-a, 11-04-00932-a, and 10-04-90062-Bel_a) and the Program "Molecular and Cell Biology" of the Presidium of the Russian Academy of Sciences.

■ ABBREVIATIONS

PEG, polyethylene glycol; TMAO, trimethylamine *N*-oxide; sHsp, small heat shock protein; Phb, glycogen phosphorylase *b*; UV, ultraviolet; AUC, analytical ultracentrifugation; SEC, size-exclusion chromatography; SDS−PAGE, sodium dodecyl sulfate−polyacrylamide gel electrophoresis; DSC, differential scanning calorimetry; DLS, dynamic light scattering; GAPDH, glyceraldehyde-3-phosphate dehydrogenase.

■ REFERENCES

(1) Hall, D., and Minton, A. P. (2003) Macromolecular crowding: Qualitative and semiquantitative successes, quantitative challenges. *Biochim. Biophys. Acta 1649*, 127−139.

(2) Chebotareva, N. A., Kurganov, B. I., and Livanova, N. B. (2004) Biochemical effects of molecular crowding. *Biochemistry (Moscow, Russ. Fed.) 69*, 1239−1251.

(3) Despa, F., Orgill, D. P., and Lee, R. C. (2005) Molecular crowding effects on protein stability. *Ann. N.Y. Acad. Sci. 1066*, 54−66.

(4) Ellis, R. J., and Minton, A. P. (2006) Protein aggregation in crowded environments. *Biol. Chem. 387*, 485−497.

(5) Chebotareva, N. A. (2007) Effect of molecular crowding on the enzymes of glycogenolysis. *Biochemistry (Moscow, Russ. Fed.) 72*, 1478−1490.

(6) Hu, Z., Jiang, J., and Rajagopalan, R. (2007) Effects of macromolecular crowding on biochemical reaction equilibria: A molecular thermodynamic perspective. *Biophys. J. 93*, 1464−1473.

(7) Zhou, H. X., Rivas, G., and Minton, A. P. (2008) Macromolecular crowding and confinement: Biochemical, biophysical, and potential physiological consequences. *Annu. Rev. Biophys. 37*, 375−397.

(8) Elcock, A. H. (2010) Models of macromolecular crowding effects and the need for quantitative comparisons with experiment. *Curr. Opin. Struct. Biol. 20*, 196−206.

(9) Ellis, R. J. (2011) Protein aggregation: Opposing effects of chaperones and crowding. In *Folding for the Synapse* (Wyttenbach, A., and O'Connor, V., Eds.) pp 9−34, Springer Science+Business Media LLC, Philadelphia.

(10) Fink, A. L. (2006) The aggregation and fibrillation of α-synuclein. *Acc. Chem. Res. 39*, 628−634.

(11) Munishkina, L. A., Ahmad, A., Fink, A. L., and Uversky, V. N. (2008) Guiding protein aggregation with macromolecular crowding. *Biochemistry 47*, 8993−9006.

(12) Li, Y., and Roberts, C. J. (2009) Lumry-Eyring nucleated-polymerization model of protein aggregation kinetics. 2. Competing growth via condensation and chain polymerization. *J. Phys. Chem. B 113*, 7020−7032.

(13) Morris, A. M., Watzky, M. A., and Finke, R. G. (2009) Protein aggregation kinetics, mechanism, and curve-fitting: A review of the literature. *Biochim. Biophys. Acta 1794*, 375−397.

(14) White, D. A., Buell, A. K., Knowles, T. P., Welland, M. E., and Dobson, C. M. (2010) Protein aggregation in crowded environments. *J. Am. Chem. Soc. 132*, 5170−5175.

(15) Kurganov, B. I., Topchieva, I. N., Lisovskaia, N. P., Chebotareva, N. A., and Natarius, O. (1979) Effect of polyethylene glycol on association of muscle phosphorylase *b*. *Biokhimiia 44*, 629−633.

(16) Winzor, D. J., and Wills, P. R. (2006) Molecular crowding effects of linear polymers in protein solutions. *Biophys. Chem. 119*, 186−195.
(17) Timasheff, S. N. (2002) Protein-solvent preferential interactions, protein hydration, and the modulation of biochemical reactions by solvent components. *Proc. Natl. Acad. Sci. U.S.A. 99*, 9721−9726.
(18) Arakawa, T., Ejima, D., Kita, Y., and Tsumoto, K. (2006) Small molecule pharmacological chaperones: From thermodynamic stabilization to pharmaceutical drugs. *Biochim. Biophys. Acta 1764*, 1677−1687.
(19) Chebotareva, N. A., Harding, S. E., and Winzor, D. J. (2001) Ultracentrifugal studies of the effect of molecular crowding by trimethylamine N-oxide on the self-association of muscle glycogen phosphorylase *b*. *Eur. J. Biochem. 268*, 506−513.
(20) Singh, R., Haque, I., and Ahmad, F. (2005) Counteracting osmolyte trimethylamine N-oxide destabilizes proteins at pH below its pK_a. Measurements of thermodynamic parameters of proteins in the presence and absence of trimethylamine N-oxide. *J. Biol. Chem. 280*, 11035−11042.
(21) Chebotareva, N. A., Meremyanin, A. V., Makeeva, V. F., Livanova, N. B., and Kurganov, B. I. (2008) Cooperative self-association of phosphorylase kinase from rabbit skeletal muscle. *Biophys. Chem. 133*, 45−53.
(22) Chebotareva, N. A., Meremyanin, A. V., Makeeva, V. F., Eronina, T. B., and Kurganov, B. I. (2009) Glycogen phosphorylase *b* and phosphorylase kinase binding to glycogen under molecular crowding conditions. Inhibitory effect of FAD. *Biochemistry (Moscow. Russ. Fed.) 74*, 562−568.
(23) Yancey, P. H., Fyfe-Johnson, A. L., Kelly, R. H., Walker, V. P., and Aunon, M. T. (2001) Trimethylamine oxide counteracts effects of hydrostatic pressure on proteins of deep-sea teleosts. *J. Exp. Zool. 289*, 172−176.
(24) Seibel, B. A., and Walsh, P. J. (2002) Trimethylamine oxide accumulation in marine animals: Relationship to acylglycerol storage. *J. Exp. Biol. 205*, 297−306.
(25) Yancey, P. H. (2005) Organic osmolytes as compatible, metabolic and counteracting cytoprotectants in high osmolarity and other stresses. *J. Exp. Biol. 208*, 2819−2830.
(26) Ganea, E. (2001) Chaperone-like activity of α-crystallin and other small heat shock proteins. *Curr. Protein Pept. Sci. 2*, 205−225.
(27) Horwitz, J. (1992) α-Crystallin can function as a molecular chaperone. *Proc. Natl. Acad. Sci. U.S.A. 89*, 10449−10453.
(28) Rao, P. V., Horwitz, J., and Zigler, J. S. Jr. (1993) α-Crystallin, a molecular chaperone, forms a stable complex with carbonic anhydrase upon heat denaturation. *Biochem. Biophys. Res. Commun. 190*, 786−793.
(29) Wang, K., and Spector, A. (1994) The chaperone activity of bovine α-crystallin. Interaction with other lens crystallins in native and denatured states. *J. Biol. Chem. 269*, 13601−13608.
(30) Bettelheim, F. A., Ansari, R., Cheng, Q. F., and Zigler, J. S. Jr. (1999) The mode of chaperoning of dithiothreitol-denatured α-lactalbumin by α-crystallin. *Biochem. Biophys. Res. Commun. 261*, 292−297.
(31) Abgar, S., Yevlampieva, N., Aerts, T., Vanhoudt, J., and Clauwaert, J. (2000) Chaperone-like activity of bovine lens α-crystallin in the presence of dithiothreitol-destabilized proteins: Characterization of the formed complexes. *Biochem. Biophys. Res. Commun. 276*, 619−625.
(32) Neal, R., Zigler, J. S. Jr., and Bettelheim, F. A. (2001) On the equilibrium between monomeric α-lactalbumin and the chaperoning complex of α-crystallin. *Biochem. Biophys. Res. Commun. 280*, 14−18.
(33) Rajaraman, K., Raman, B., Ramakrishna, T., and Rao, C. M. (2001) Interaction of human recombinant αA- and αB-crystallins with early and late unfolding intermediates of citrate synthase on its thermal denaturation. *FEBS Lett. 497*, 118−123.
(34) Devlin, G. L., Carver, J. A., and Bottomley, S. P. (2003) The selective inhibition of serpin aggregation by the molecular chaperone, α-crystallin, indicates a nucleation-dependent specificity. *J. Biol. Chem. 278*, 48644−48650.
(35) Krivandin, A. V., Muranov, K. O., and Ostrovskii, M. A. (2004) Studies of α- and βL-crystallin complex formation in solution at 60 °C. *Mol. Biol. (Moscow) 38*, 532−546.
(36) Krivandin, A. V., Muranov, K. O., and Ostrovsky, M. A. (2004) Heat-induced complex formation in solutions of α- and βL-crystallins: A small-angle X-ray scattering study. *Dokl. Biochem. Biophys. 394*, 1−4.
(37) Bumagina, Z. M., Gurvits, B. Y., Artemova, N. V., Muranov, K. O., Yudin, I. K., and Kurganov, B. I. (2010) Mechanism of suppression of dithiothreitol-induced aggregation of bovine α-lactalbumin by α-crystallin. *Biophys. Chem. 146*, 108−117.
(38) Regini, J. W., Ecroyd, H., Meehan, S., Bremmell, K., Clarke, M. J., Lammie, D., Wess, T., and Carver, J. A. (2010) The interaction of unfolding α-lactalbumin and malate dehydrogenase with the molecular chaperone αB-crystallin: A light and X-ray scattering investigation. *Mol. Vision 16*, 2446−2456.
(39) Khanova, H. A., Markossian, K. A., Kurganov, B. I., Samoilov, A. M., Kleimenov, S. Y., Levitsky, D. I., Yudin, I. K., Timofeeva, A. C., Muranov, K. O., and Ostrovsky, M. A. (2005) Mechanism of chaperone-like activity. Suppression of thermal aggregation of βL-crystallin by α-crystallin. *Biochemistry 44*, 15480−15487.
(40) Markossian, K. A., Khanova, H. A., Kleimenov, S. Y., Levitsky, D. I., Chebotareva, N. A., Asryants, R. A., Muronetz, V. I., Saso, L., Yudin, I. K., and Kurganov, B. I. (2006) Mechanism of thermal aggregation of rabbit muscle glyceraldehyde-3-phosphate dehydrogenase. *Biochemistry 45*, 13375−13384.
(41) Brockwell, C. H. (2009) The effect of pH on the structure and function of α-crystallin and cyclodextrins as artificial molecular chaperones. Ph.D. Thesis, University of Adelaide, Adelaide, Australia.
(42) Ganea, E., and Harding, J. J. (2002) The effect of macromolecular crowding on chaperone activity of α-crystallin. *Proc. Rom. Acad., Ser. B: Chem., Life Sci. Geosci. 1*, 13−17.
(43) Ghahghaei, A., Rekas, A., Price, W. E., and Carver, J. A. (2007) The effect of dextran on subunit exchange of the molecular chaperone αA-crystallin. *Biochim. Biophys. Acta 1774*, 102−111.
(44) Ghahghaei, A., Divsalar, A., and Faridi, N. (2010) The effects of molecular crowding on the amyloid fibril formation of α-lactalbumin and the chaperone action of α-casein. *Protein J. 29*, 257−264.
(45) Fischer, E. H., and Krebs, E. G. (1962) Muscle phosphorylase *b*. *Methods Enzymol. 5*, 369−373.
(46) Kastenschmidt, L. L., Kastenschmidt, J., and Helmreich, E. (1968) Subunit interactions and their relationship to the allosteric properties of rabbit skeletal muscle phosphorylase *b*. *Biochemistry 7*, 3590−3608.
(47) Chiou, S. H., Azari, P., Himmel, M. E., and Squire, P. G. (1979) Isolation and physical characterization of bovine lens crystallins. *Int. J. Pept. Protein Res. 13*, 409−417.
(48) Putilina, T., Skouri-Panet, F., Prat, K., Lubsen, N. H., and Tardieu, A. (2003) Subunit exchange demonstrates a differential chaperone activity of calf α-crystallin toward βL- and individual γ-crystallins. *J. Biol. Chem. 278*, 13747−13756.
(49) Sugrobova, N. P., Lisovskaia, N. P., and Kurganov, B. I. (1982) Determination of glycogen phosphorylase B activity by the turbidimetric method in the presence of the forward and reverse reaction substrates. *Biokhimiia 47*, 1883−1888.
(50) Sugrobova, N. P., Lisovskaja, N. P., and Kurganov, B. I. (1983) Turbidimetric method for determination of glycogen phosphorylase activity and its use for estimation of equilibrium position of enzymic reaction. *J. Biochem. Biophys. Methods 8*, 299−306.
(51) Kurganov, B. I. (2002) Estimation of the activity of molecular chaperones in test-systems based on suppression of protein aggregation. *Usp. Biol. Khim. 42*, 89−138.
(52) Kurganov, B. I. (2002) Kinetics of protein aggregation. Quantitative estimation of the chaperone-like activity in test-systems based on suppression of protein aggregation. *Biochemistry (Moscow, Russ. Fed.) 67*, 409−422.
(53) Kurganov, B. I. (2005) Protein aggregation kinetics. In *Chemical and Biological Kinetics. New Horizons. Volume 2: Biological Kinetics* (Burlakova, E. B., and Varfolomeev, S. D., Eds.) pp 251−279, Koninklijke Brill NV, Leiden, The Netherlands.

(54) Wang, K., and Kurganov, B. I. (2003) Kinetics of heat- and acidification-induced aggregation of firefly luciferase. *Biophys. Chem. 106*, 97−109.
(55) Schuck, P., and Rossmanith, P. (2000) Determination of the sedimentation coefficient distribution by least-squares boundary modeling. *Biopolymers 54*, 328−341.
(56) Brown, P. H., and Schuck, P. (2006) Macromolecular size-and-shape distributions by sedimentation velocity analytical ultracentrifugation. *Biophys. J. 90*, 4651−4661.
(57) Laemmli, U. K. (1970) Cleavage of structural proteins during the assembly of the head of bacteriophage T4. *Nature 227*, 680−685.
(58) *Scientist for experimental data fitting, Microsoft Windows version 2.0* (1995) MicroMath, Inc., Salt Lake City.
(59) Setlow, R., and Doyle, B. (1954) The effect of temperature on the ultraviolet light inactivation of trypsin. *Arch. Biochem. Biophys. 48*, 441−447.
(60) Setlow, R., and Doyle, B. (1957) The action of monochromatic ultraviolet light on proteins. *Biochim. Biophys. Acta 24*, 27−41.
(61) Vladimirov, Y. A. (1965) *Photochemistry and Luminescence of Proteins*, Nauka, Moscow.
(62) Kurganov, B. I., Kornilaev, B. A., Chebotareva, N. A., Malikov, V. P., Orlov, V. N., Lyubarev, A. E., and Livanova, N. B. (2000) Dissociative mechanism of thermal denaturation of rabbit skeletal muscle glycogen phosphorylase *b*. *Biochemistry 39*, 13144−13152.
(63) International Standard ISO 22412:2008(E). Particle size analysis−Dynamic light scattering (DLS) (2008) International Organization for Standardization, Geneva.
(64) Gunar, V. I., Sugrobova, N. P., Chebotareva, N. A., Stepanova, S. V., Poznanskaya, A. A., and Kurganov, B. I. (1991) Synthesis of pyridoxal-5′-phosphate analogs and their interaction with apoenzyme of glycogen phosphorylase *b*. In *Enzymes Dependent on Pyridoxal Phosphate and Other Carbonyl Components as Cofactors* (Fukui, T., Kagamiyama, H., Soda, K., and Wada, H., Eds.) pp 417−419, Pergamon Press, Oxford, U.K.
(65) Meremyanin, A. V., Eronina, T. B., Chebotareva, N. A., Kleimenov, S. Y., Yudin, I. K., Muranov, K. O., Ostrovsky, M. A., and Kurganov, B. I. (2007) Effect of α-crystallin on thermal aggregation of glycogen phosphorylase *b* from rabbit skeletal muscle. *Biochemistry (Moscow, Russ. Fed.) 72*, 518−528.
(66) Philo, J. S. (2006) Is any measurement method optimal for all aggregate sizes and types? *AAPS J. 8*, E564−E571.
(67) Philo, J. S. (2009) A critical review of methods for size characterization of non-particulate protein aggregates. *Curr. Pharm. Biotechnol. 10*, 359−372.
(68) Yousefi, R., Shchutskaya, Y. Y., Zimny, J., Gaudin, J. C., Moosavi-Movahedi, A. A., Muronetz, V. I., Zuev, Y. F., Chobert, J. M., and Haertle, T. (2009) Chaperone-like activities of different molecular forms of β-casein. Importance of polarity of N-terminal hydrophilic domain. *Biopolymers 91*, 623−632.
(69) Khalili-Hezarjaribi, H., Yousefi, R., and Moosavi-Movahedi, A. A. (2011) Effect of temperature and ionic strength on structure and chaperone activity of glycated and non-glycated α-crystallins. *Protein Pept. Lett.*, PubMed ID: 21933131.
(70) Yousefi, R., and Jalili, S. (2011) The synergistic chaperoning operation in a Bi-chaperone system consisting of α-crystallin and β-casein: Bovine pancreatic insulin as the target protein. *Colloids Surf., B 88*, 497−504.
(71) Hamada, D., and Dobson, C. M. (2002) A kinetic study of β-lactoglobulin amyloid fibril formation promoted by urea. *Protein Sci. 11*, 2417−2426.
(72) Shinozaki, K., Konakahara, T., Okuno, H., and Kodaka, M. (2003) Analysis of fibril formation of amyloid-β-protein by stretched exponential function. *Protein Pept. Lett. 10*, 569−574.
(73) Kudou, M., Shiraki, K., and Takagi, M. (2005) Stretched-exponential analysis of heat-induced aggregation of apo-concanavalin A. *Protein J. 24*, 193−199.
(74) Stirpe, A., Pantusa, M., Rizzuti, B., Sportelli, L., Bartucci, R., and Guzzi, R. (2011) Early stage aggregation of human serum albumin in the presence of metal ions. *Int. J. Biol. Macromol. 49*, 337−342.
(75) Vetri, V., D'Amico, M., Fodera, V., Leone, M., Ponzoni, A., Sberveglieri, G., and Militello, V. (2011) Bovine serum albumin protofibril-like aggregates formation: Solo but not simple mechanism. *Arch. Biochem. Biophys. 508*, 13−24.
(76) Muranov, K. O., Maloletkina, O. I., Poliansky, N. B., Markossian, K. A., Kleymenov, S. Y., Rozhkov, S. P., Goryunov, A. S., Ostrovsky, M. A., and Kurganov, B. I. (2011) Mechanism of aggregation of UV-irradiated β_L-crystallin. *Exp. Eye Res. 92*, 76−86.
(77) Lindner, R. A., Treweek, T. M., and Carver, J. A. (2001) The molecular chaperone α-crystallin is in kinetic competition with aggregation to stabilize a monomeric molten-globule form of α-lactalbumin. *Biochem. J. 354*, 79−87.
(78) Raman, B., and Rao, C. M. (1994) Chaperone-like activity and quaternary structure of α-crystallin. *J. Biol. Chem. 269*, 27264−27268.
(79) Das, K. P., and Surewicz, W. K. (1995) Temperature-induced exposure of hydrophobic surfaces and its effect on the chaperone activity of α-crystallin. *FEBS Lett. 369*, 321−325.
(80) Raman, B., Ramakrishna, T., and Rao, C. M. (1995) Temperature dependent chaperone-like activity of α-crystallin. *FEBS Lett. 365*, 133−136.
(81) Raman, B., and Rao, C. M. (1997) Chaperone-like activity and temperature-induced structural changes of α-crystallin. *J. Biol. Chem. 272*, 23559−23564.
(82) Reddy, G. B., Das, K. P., Petrash, J. M., and Surewicz, W. K. (2000) Temperature-dependent chaperone activity and structural properties of human αA- and αB-crystallins. *J. Biol. Chem. 275*, 4565−4570.
(83) Weiss, W. F. IV, Young, T. M., and Roberts, C. J. (2009) Principles, approaches, and challenges for predicting protein aggregation rates and shelf life. *J. Pharm. Sci. 98*, 1246−1277.
(84) Ferrone, F. (2003) Analysis of protein aggregation kinetics. *Methods Enzymol. 309*, 256−274.
(85) Golub, N., Meremyanin, A., Markossian, K., Eronina, T., Chebotareva, N., Asryants, R., Muronets, V., and Kurganov, B. (2007) Evidence for the formation of start aggregates as an initial stage of protein aggregation. *FEBS Lett. 581*, 4223−4227.
(86) Panyukov, Y., Yudin, I., Drachev, V., Dobrov, E., and Kurganov, B. (2007) The study of amorphous aggregation of tobacco mosaic virus coat protein by dynamic light scattering. *Biophys. Chem. 127*, 9−18.
(87) Markossian, K. A., Golub, N. V., Khanova, H. A., Levitsky, D. I., Poliansky, N. B., Muranov, K. O., and Kurganov, B. I. (2008) Mechanism of thermal aggregation of yeast alcohol dehydrogenase I: Role of intramolecular chaperone. *Biochim. Biophys. Acta 1784*, 1286−1293.
(88) Meremyanin, A. V., Eronina, T. B., Chebotareva, N. A., and Kurganov, B. I. (2008) Kinetics of thermal aggregation of glycogen phosphorylase *b* from rabbit skeletal muscle: Mechanism of protective action of α-crystallin. *Biopolymers 89*, 124−134.
(89) Golub, N. V., Markossian, K. A., Sholukh, M. V., Muranov, K. O., and Kurganov, B. I. (2009) Study of kinetics of thermal aggregation of mitochondrial aspartate aminotransferase by dynamic light scattering: Protective effect of α-crystallin. *Eur. Biophys. J. 38*, 547−556.
(90) Markossian, K. A., Yudin, I. K., and Kurganov, B. I. (2009) Mechanism of suppression of protein aggregation by α-crystallin. *Int. J. Mol. Sci. 10*, 1314−1345.
(91) Eronina, T. B., Chebotareva, N. A., Bazhina, S. G., Kleymenov, S. Y., Naletova, I. N., Muronetz, V. I., and Kurganov, B. I. (2010) Effect of GroEL on thermal aggregation of glycogen phosphorylase *b* from rabbit skeletal muscle. *Macromol. Biosci. 10*, 768−774.
(92) Eronina, T. B., Chebotareva, N. A., Kleymenov, S. Y., Roman, S. G., Makeeva, V. F., and Kurganov, B. I. (2010) Effect of 2-hydroxypropyl-β-cyclodextrin on thermal stability and aggregation of glycogen phosphorylase *b* from rabbit skeletal muscle. *Biopolymers 93*, 986−993.
(93) Maloletkina, O. I., Markossian, K. A., Asryants, R. A., Semenyuk, P. I., Makeeva, V. F., and Kurganov, B. I. (2010) Effect of 2-hydroxypropyl-β-cyclodextrin on thermal inactivation, denaturation

and aggregation of glyceraldehyde-3-phosphate dehydrogenase from rabbit skeletal muscle. *Int. J. Biol. Macromol. 46*, 487−492.
(94) Maloletkina, O. I., Markossian, K. A., Belousova, L. V., Kleimenov, S. Y., Orlov, V. N., Makeeva, V. F., and Kurganov, B. I. (2010) Thermal stability and aggregation of creatine kinase from rabbit skeletal muscle. Effect of 2-hydroxypropyl-β-cyclodextrin. *Biophys. Chem. 148*, 121−130.
(95) Markossian, K. A., Golub, N. V., Chebotareva, N. A., Asryants, R. A., Naletova, I. N., Muronetz, V. I., Muranov, K. O., and Kurganov, B. I. (2010) Comparative analysis of the effects of α-crystallin and GroEL on the kinetics of thermal aggregation of rabbit muscle glyceraldehyde-3-phosphate dehydrogenase. *Protein J. 29*, 11−25.
(96) Markossian, K. A., Kurganov, B. I., Levitsky, D. I., Khanova, H. A., Chebotareva, N. A., Samoilov, A. M., Eronina, T. B., Fedurkina, N. V., Mitskevich, L. G., Merem'yanin, A. V., Kleymenov, S. Yu., Makeeva, V. F., Muronets, V. I., Naletova, I. N., Shalova, I. N., Asryants, R. A., Schmalhausen, E. V., Saso, L., Panyukov, Yu. V., Dobrov, E. N., Yudin, I. K., Timofeeva, A. C., Muranov, K. O., and Ostrovsky, M. A. (2006) Mechanisms of chaperone-like activity. In *Protein Folding: New Research* (Obalinsky, T. R., Ed.) pp 89−171, Nova Science Publishers Inc., New York.
(97) Kurganov, B. I. (1998) Kinetics of heat aggregation of proteins. *Biochemistry (Moscow, Russ. Fed.) 63*, 364−366.
(98) Eronina, T. B., Chebotareva, N. A., Bazhina, S. G., Makeeva, V. F., Kleymenov, S. Y., and Kurganov, B. I. (2009) Effect of proline on thermal inactivation, denaturation and aggregation of glycogen phosphorylase *b* from rabbit skeletal muscle. *Biophys. Chem. 141*, 66−74.
(99) Khanova, H. A., Markossian, K. A., Kleimenov, S. Y., Levitsky, D. I., Chebotareva, N. A., Golub, N. V., Asryants, R. A., Muronetz, V. I., Saso, L., Yudin, I. K., Muranov, K. O., Ostrovsky, M. A., and Kurganov, B. I. (2007) Effect of α-crystallin on thermal denaturation and aggregation of rabbit muscle glyceraldehyde-3-phosphate dehydrogenase. *Biophys. Chem. 125*, 521−531.
(100) Chebotareva, N. A., Kurganov, B. I., Muranov, K. O., Asryants, R. A., and Ostrovsky, M. A. (2009) Role of thermoinduced dissociation in interaction between α-crystallin as an oligomeric chaperone and glyceraldehyde-3-phosphate dehydrogenase as an oligomeric protein substrate. *Dokl. Biochem. Biophys. 428*, 245−248.
(101) Weitz, D. A., and Lin, M. Y. (1986) Dynamic scaling of cluster-mass distributions in kinetic colloid aggregation. *Phys. Rev. Lett. 57*, 2037−2040.
(102) van den Oetelaar, P. J., van Someren, P. F., Thomson, J. A., Siezen, R. J., and Hoenders, H. J. (1990) A dynamic quaternary structure of bovine α-crystallin as indicated from intermolecular exchange of subunits. *Biochemistry 29*, 3488−3493.
(103) Bova, M. P., Ding, L. L., Horwitz, J., and Fung, B. K. (1997) Subunit exchange of αA-crystallin. *J. Biol. Chem. 272*, 29511−29517.
(104) Bova, M. P., McHaourab, H. S., Han, Y., and Fung, B. K. (2000) Subunit exchange of small heat shock proteins. Analysis of oligomer formation of αA-crystallin and Hsp27 by fluorescence resonance energy transfer and site-directed truncations. *J. Biol. Chem. 275*, 1035−1042.
(105) Datta, S. A., and Rao, C. M. (2000) Packing-induced conformational and functional changes in the subunits of α-crystallin. *J. Biol. Chem. 275*, 41004−41010.
(106) Liu, L., Ghosh, J. G., Clark, J. I., and Jiang, S. (2006) Studies of αB-crystallin subunit dynamics by surface plasmon resonance. *Anal. Biochem. 350*, 186−195.
(107) Krushelnitsky, A., Mukhametshina, N., Gogolev, Y., Tarasova, N., Faizullin, D., Zinkevich, T., Gnezdilov, O., and Fedotov, V. (2008) Subunit mobility and the chaperone activity of recombinant αB-crystallin. *Open Biochem. J. 2*, 116−120.
(108) Carver, J. A., Rekas, A., Thorn, D. C., and Wilson, M. R. (2003) Small heat-shock proteins and clusterin: Intra- and extracellular molecular chaperones with a common mechanism of action and function? *IUBMB Life 55*, 661−668.
(109) Ecroyd, H., and Carver, J. A. (2009) Crystallin proteins and amyloid fibrils. *Cell. Mol. Life Sci. 66*, 62−81.
(110) Sun, Y., and MacRae, T. H. (2005) Small heat shock proteins: Molecular structure and chaperone function. *Cell. Mol. Life Sci. 62*, 2460−2476.
(111) Haslbeck, M., Walke, S., Stromer, T., Ehrnsperger, M., White, H. E., Chen, S., Saibil, H. R., and Buchner, J. (1999) Hsp26: A temperature-regulated chaperone. *EMBO J. 18*, 6744−6751.
(112) Gu, L., Abulimiti, A., Li, W., and Chang, Z. (2002) Monodisperse Hsp16.3 nonamer exhibits dynamic dissociation and reassociation, with the nonamer dissociation prerequisite for chaperone-like activity. *J. Mol. Biol. 319*, 517−526.
(113) Fu, X., Liu, C., Liu, Y., Feng, X., Gu, L., Chen, X., and Chang, Z. (2003) Small heat shock protein Hsp16.3 modulates its chaperone activity by adjusting the rate of oligomeric dissociation. *Biochem. Biophys. Res. Commun. 310*, 412−420.
(114) Fu, X., and Chang, Z. (2004) Temperature-dependent subunit exchange and chaperone-like activities of Hsp16.3, a small heat shock protein from *Mycobacterium tuberculosis*. *Biochem. Biophys. Res. Commun. 316*, 291−299.
(115) Shashidharamurthy, R., Koteiche, H. A., Dong, J., and McHaourab, H. S. (2005) Mechanism of chaperone function in small heat shock proteins: Dissociation of the HSP27 oligomer is required for recognition and binding of destabilized T4 lysozyme. *J. Biol. Chem. 280*, 5281−5289.
(116) Kocabiyik, S. (2009) Essential structural and functional features of small heat shock proteins in molecular chaperoning process. *Protein Pept. Lett. 16*, 613−622.
(117) Stengel, F., Baldwin, A. J., Painter, A. J., Jaya, N., Basha, E., Kay, L. E., Vierling, E., Robinson, C. V., and Benesch, J. L. (2010) Quaternary dynamics and plasticity underlie small heat shock protein chaperone function. *Proc. Natl. Acad. Sci. U.S.A. 107*, 2007−2012.
(118) Jiao, W., Li, P., Zhang, J., Zhang, H., and Chang, Z. (2005) Small heat-shock proteins function in the insoluble protein complex. *Biochem. Biophys. Res. Commun. 335*, 227−231.
(119) Chebotareva, N. A., Makeeva, V. F., Bazhina, S. G., Eronina, T. B., Gusev, N. B., and Kurganov, B. I. (2010) Interaction of Hsp27 with native phosphorylase kinase under crowding conditions. *Macromol. Biosci. 10*, 783−789.

Supporting information

Does the Crowded Cell-like Environment Reduce the Chaperone-like Activity of α-Crystallin?

Svetlana G. Roman, Natalia A. Chebotareva, Tatyana B. Eronina, Sergey Yu. Kleymenov, Valentina F. Makeeva, Nikolay B. Poliansky, Konstantin O. Muranov, Boris I. Kurganov

Table S1: The Values of Refractive Index (*n*), Density (ρ) and Dynamic Viscosity (η) of Solutions of PEG-20000, Ficoll-70000 and TMAO at 20 °C (80 mM Hepes pH 6.8, Containing 100 mM NaCl)

Concentration	*n*	ρ, g·cm^{-3}	η, mPa·s
PEG-20000			
20 mg·mL^{-1}	1.338	1.01211	2.1350
30 mg·mL^{-1}	1.339	1.01385	2.9404
Ficoll-70000			
100 mg·mL^{-1}	1.350	1.04307	3.1787
125 mg·mL^{-1}	1.353	1.05121	4.0969
200 mg·mL^{-1}	1.365	1.07563	8.6747
TMAO			
0.5 M	1.339	1.01022	1.2113
0.75 M	1.342	1.01062	1.3150

1 M	1.344	1.01133	1.4087

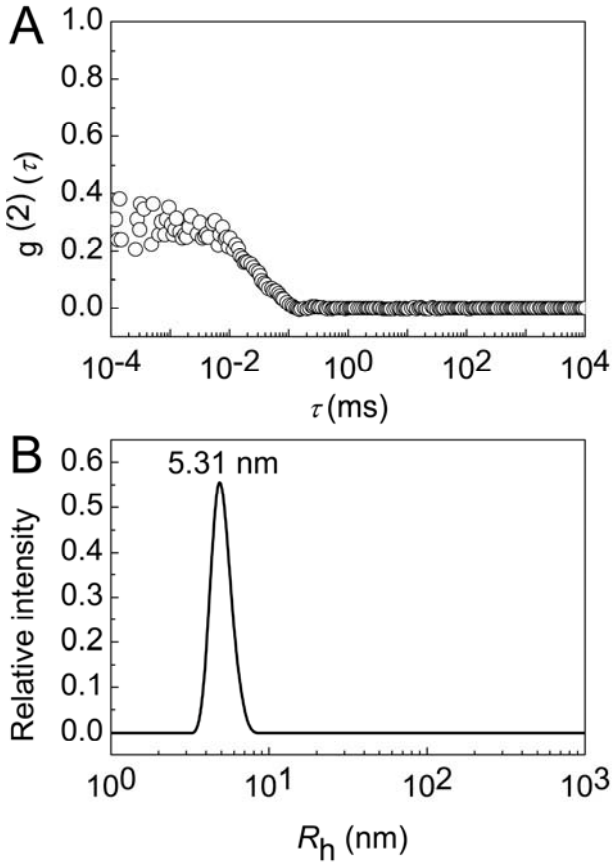

Figure S1. The autocorrelation function (A) and the particle size distribution (B) obtained by DLS measurements for native Ph*b* (2 mg·mL^{-1}) at 20 °C.

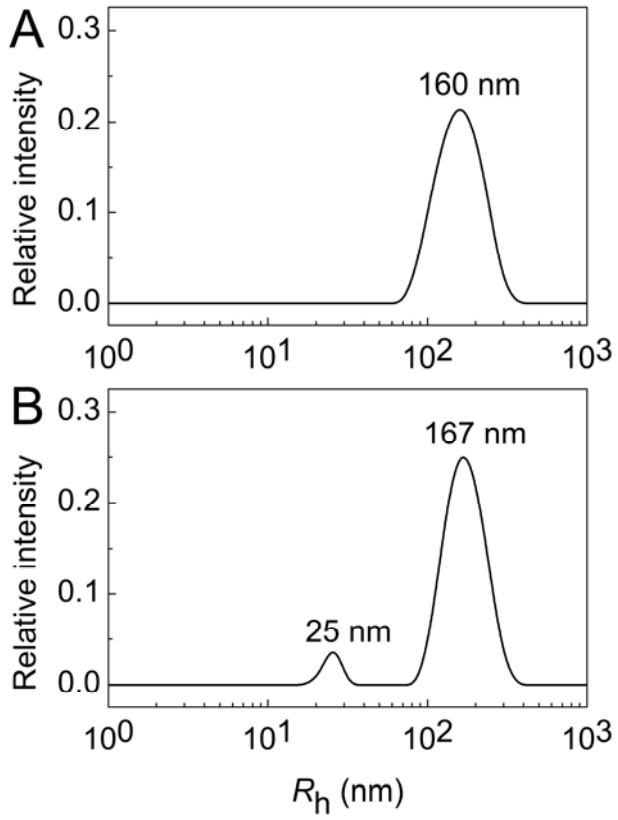

Figure S2. The particle size distributions registered for UV-irradiated Ph*b* (0.15 mg·mL^{-1}) heated at 37 °C for 35 min in the absence of α-crystallin (A) and for 400 min in the presence of α-crystallin at the concentration of 0.15 mg·mL^{-1} (B).

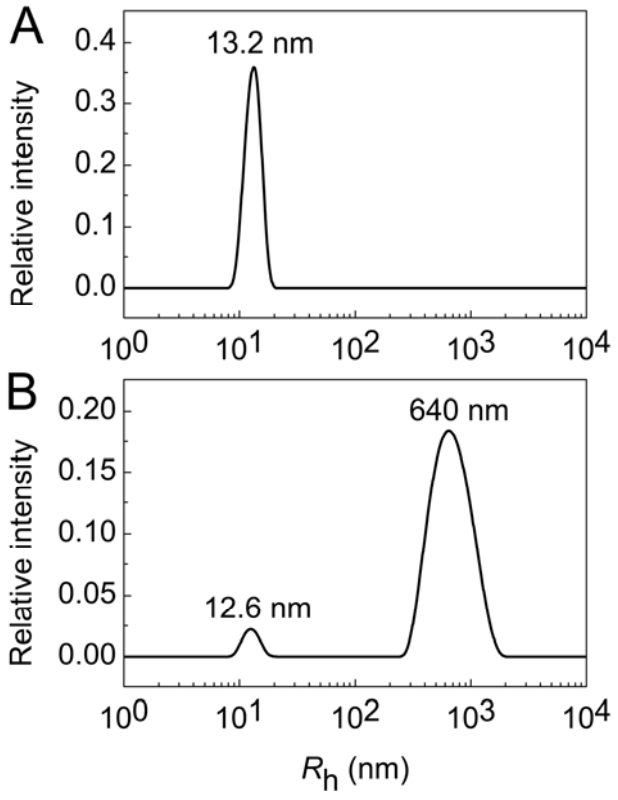

Figure S3. The particle size distributions registered at 37 °C for the mixture of UV-irradiated Ph*b* (0.15 mg·mL^{-1}) and α-crystallin (1.5 mg·mL^{-1}) before the addition of PEG-20000 (A) and within 3 minutes after the addition of PEG-20000 at the final concentration of 30 mg·mL^{-1}.

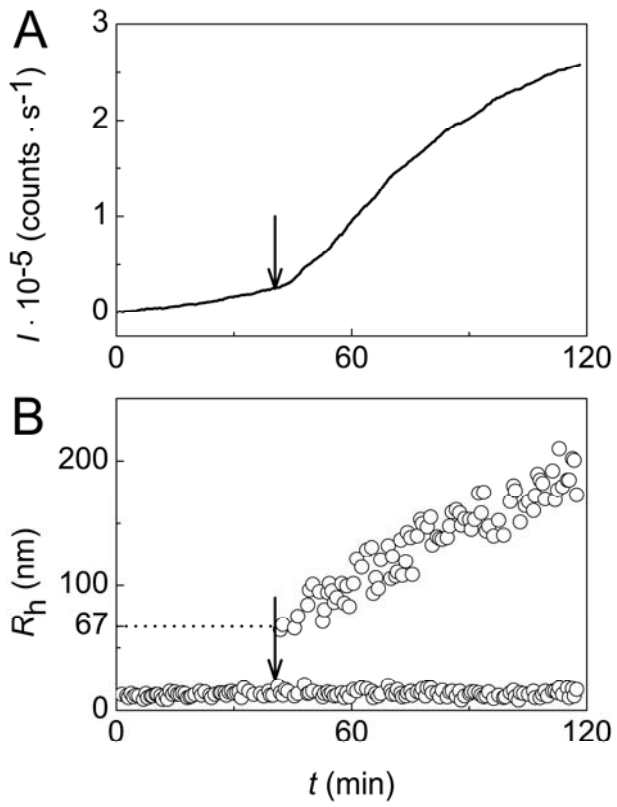

Figure S4. PEG-induced aggregation of Ph*b* in the system UV-irradiated Ph*b* (0.15 mg·mL^{-1})+α-crystallin (1.5 mg·mL^{-1}) at 35 °C. The dependences of the light scattering intensity and the hydrodynamic radii of the particles on time (panels A and B, respectively). The arrow points the moment of the addition of PEG-20000 (10 mg·mL^{-1}).

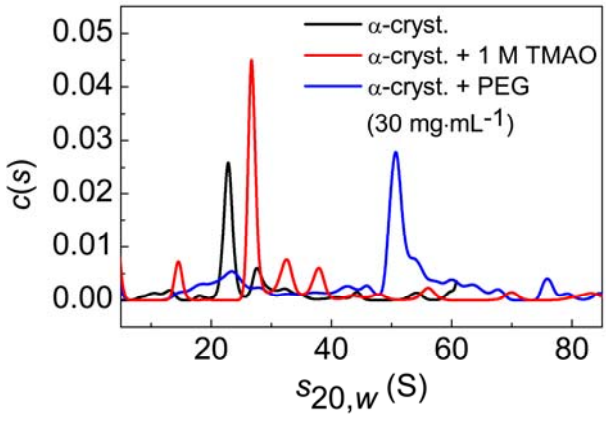

Figure S5. Sedimentation behavior of α-crystallin (0.2 mg·mL^{-1}) in the absence and the presence of crowding agents (1 M TMAO or PEG-20000 at the concentration of 30 mg·mL^{-1}) at 37 °C. Before centrifugation samples were heated for 5 h at 37 °C. Rotor speed was 40000 rpm. Sedimentation coefficient distributions $c(s)$ obtained at 37 °C were transformed to standard $s_{20,w}$-distributions.